New microfossil and strontium isotope chronology used to identify the controls of Miocene reefs and related facies in NW Cyprus

New microfossil and strontium isotope chronology used to identify the controls of Miocene reefs and related facies in NW Cyprus

Torin Cannings*[1], Elizabeth M. Balmer[1], Giovanni Coletti[2], Ryan B. Ickert[3,4], Dick Kroon[1], Isabella Raffi[5] & Alastair H.F. Robertson[1]

[1]*School of GeoSciences, Grant Institute, University of Edinburgh, James Hutton Road, Edinburgh EH9 3FE, UK*
[2] *Dipartimento di Scienze dell'Ambiente e del Territorio e di Scienze della Terra, Università di Milano-Bicocca, 20126, Milano, Italy*
[3]*Scottish Universities Environmental Research Centre, Scottish Enterprise Technology Park, Rankine Avenue, East Kilbride, G75 0QF*
[4]*Department of Earth, Atmospheric, and Planetary Sciences, Purdue University. West Lafayette, IN, 47907. (present affiliation)*
[5]*Dipartimento di Ingegneria e Geotecnologie (InGeo), CeRSGeoUniversità degli Studi 'G. d'Annunzio' di Chieti-Pescara Campus Universitario, via dei Vestini 31 66013 Chieti Scalo, Italy*
*Correspondence (torin.cannings@ed.ac.uk)

Abbreviated Title - Miocene reefs and related facies in NW Cyprus

The existing chronostratigraphic framework in NW Cyprus of two-phase, Early and Late Miocene reef and associated facies development is tested and improved using a combination of calcareous nannofossil, benthic and planktic foraminiferal, and also Sr isotope dating. Following localised Late Oligocene neritic carbonate deposition (e.g. benthic foraminiferal shoals), reefs and related facies (Terra Member) began to develop *c.* 24 Ma (Aquitanian) and terminated *c.* 16 Ma (end-Burdigalian). Early Miocene reef and marginal facies were then extensively redeposited as multiple debris-flow deposits until *c.* 13.7 Ma, influenced by a combination of global sea-level fall (related to growth of the East Antarctic Ice Sheet) and local- to regional-scale tectonics. Reef growth and related deposition resumed (Koronia Member) *c.* 9.1 Ma (Tortonian), then terminated by *c.* 6.1 Ma (mid-Messinian), followed by the Messinian salinity crisis. Neritic accumulation in NW Cyprus began earlier (Late Oligocene), than in southern Cyprus (Early Miocene). The Early Miocene reefs developed on a *c.* N-S-trending structural high in the west (Akamas Peninsula area) whereas the Late Miocene reefs developed on both flanks of the neotectonic Polis graben. The two-phase reef development is mirrored in SE Cyprus and in some other Mediterranean areas; e.g. S Turkey, Israel, Italy, S Spain.

Key words: NW Cyprus, Miocene, Terra Member, Koronia Member, Polis graben, sea-level change, climate change.

Supplementary material: GPS Locations of dated samples, the Sr isotope method and the samples examined for planktic foraminifera biostratigraphy are available at https://doi.org/xxxx.

The Miocene of the Mediterranean was a time of changing tectonic setting, climate and eustatic sea level (e.g. Hüsing *et al.,* 2009; Robertson *et al.,* 2012; Herold *et al.,* 2012). The global climate cooled slightly during the Early Miocene, followed by major warming (~4 ºC rise) related to the onset of the Middle Miocene Climate Optimum (MMCO) (*c.* 17 Ma) (Zachos *et al.,* 2001; Westerhold *et al.,* 2005; Zachos *et al.,* 2008; Miller *et al.,* 2020). The MMCO was followed (*c.* 14.8 Ma) by three-step cooling related to the Middle Miocene Climate Transition (MMCT), after which the global and Mediterranean climates are believed to have remained relatively cool (Kennett *et al.,* 1975; Flower & Kennett, 1994; Holbourn *et al.,* 2005; Miller *et al.,* 2005; John *et al.,* 2011; Miller *et al.,* 2020). The global changes are likely to have influenced the Mediterranean to some extent, including the nucleation, growth and demise of coral reefs. However, the effects of the MMCO, especially on reef-building organisms in the Mediterranean remains unclear (Bosellini & Perrin 2008).

During the Early to Middle Miocene, the Eastern Mediterranean Sea was influenced by the closure of the Southern Neotethys and the collision of the Arabian and Tauride continental units in SE Turkey-Iran. This resulted in a reduction and eventual loss of the marine connection between the Southern Neotethys and the Indian Ocean (Hüsing *et al.*, 2009; Robertson *et al.*, 2012, 2016). During the Late Miocene, the connection between the W Mediterranean and the Atlantic Ocean was also lost, resulting in the Late Miocene (Messinian) salinity crisis (Hsü *et al.*, 1973; Meilijson *et al.*, 2019).

Coral reefs and associated carbonate facies are key indicators of environmental change (Kleypas *et al.*, 2001; Kiessling, 2009). Miocene reefs developed in many areas of the Mediterranean (Esteban, 1979, 1996; Franseen *et al.*, 1996; Perrin & Bosellini, 2012) (Fig. 1), including: Cyprus (e.g. Eaton & Robertson, 1993; Follows, 1992), Crete (e.g. Brachert *et al.*, 2006), Israel (e.g. Buchbinder *et al.*, 1993), S Turkey (e.g. Janson *et al.*, 2010; Pomar *et al.*, 2012; Vescogni *et al.*, 2014), S Spain (e.g. Brachert *et al.*, 1996; Pomar *et al.*, 1996; Braga & Aguirre, 2001), Corsica and Sardinia (e.g. Benisek *et al.*, 2009; Tommasetti *et al.*, 2013), Northern Italy (e.g. Chevalier, 1962); Central Italy (e.g. Bossio *et al.*, 1996); S Italy (e.g. Bosellini *et al.*, 2001; Bosellini *et al.*, 2002; Bosellini, 2006; Braga *et al.*, 2009; Pomar *et al.*, 2012), Malta (e.g. Pedley, 1979) and N Africa (e.g. Esteban, 1979, 1996; Saint Martin & Rouchy, 1990). An understanding of reef growth and demise throughout the Mediterranean is dependent on robust age controls that can be obtained using a combination of biostratigraphy and Sr isotopes, as undertaken here.

Miocene coral reefs and related facies are exposed around the northern, eastern and western margins of the Late Cretaceous Troodos ophiolitic massif (Henson *et al.*, 1949, Bagnall, 1960; Bear, 1960; Gass, 1960; Morel, 1960; Gass & Masson-Smith, 1963; Robertson, 1977a)

(Fig. 2). Previous research has shown that two phases of reef development existed, based mainly on evidence from SE and NW Cyprus, namely the Early Miocene Terra Member and the Late Miocene Koronia Member of the Miocene Pakhna Formation (Follows & Robertson, 1990; Follows, 1992; Follows *et al.*, 1996) (see below). The Early Miocene phase of reef development and related facies is best developed in SE Cyprus, near Cape Greco. Late Miocene reef and related facies are exposed *c.* 10 km to the west, near Cape Pyla (Constantinou, 1995; Follows, 1992). Here, we focus on the Early and Late Miocene reefs and related facies exposed in the less-known but important area of NW Cyprus (Fig. 1).

Our main objective here is to develop an improved chronostratigraphy for the Miocene reef-related deposits of NW Cyprus that can be used to shed light on reef growth and demise. We utilise a combination of biostratigraphy based on calcareous nannofossils, benthic foraminifera and planktic foraminifera, together with chemostratigraphy utilising Sr isotopes. Our specific aims are: (1) To improve the stratigraphy as depicted on the geological map of NW Cyprus (Constantinou, 1995); (2) To understand better the timing of the two phases of Miocene reef and reef-related facies; (3) To make chronostratigraphically-based comparisons of the dated facies in NW Cyprus with the Miocene reefs and related facies in SE Cyprus and elsewhere in the Mediterranean region, and (4) To assess the likely controls of the two-phase reef and related facies development. This is part of a wider study of the sedimentary development of the latest Cretaceous-Cenozoic of west Cyprus, currently being undertaken by the second author (Balmer).

Regional geological setting

Southern Cyprus is dominated by the Troodos ophiolite that formed by Supra-Subduction Zone spreading during the Late Cretaceous, *c.* 90 Ma (e.g. Pearce & Robinson, 2010). In our main area of interest, NW Cyprus, the crustal 'basement' beneath the Cenozoic stratigraphy was formed during the latest Cretaceous by the tectonic juxtaposition of the Late Cretaceous ophiolite with the Mesozoic continental margin/oceanic lithologies of the Mamonia Complex (e.g. Robertson & Xenophontos, 1993). This was accompanied by localised accumulation of Maastrichtian-aged polymict debris-flow deposits (Kathikas Formation) (Swarbrick & Naylor, 1980) (Fig. 3). The pre-Cenozoic 'basement' includes Early Campanian to Mid-Maastrichtian-aged volcaniclastic sedimentary rocks of the Kannaviou Formation (Robertson, 1977b; Chen & Robertson, 2019). Maastrichtian-Paleogene pelagic carbonates of the overlying Lefkara Formation are mapped in the south of the area (Fig. 3), whereas Miocene marine carbonates of the Pakhna Formation are developed more widely throughout western Cyprus (Constantinou, 1995). Pliocene-Early Pleistocene marine sediments are mainly exposed within a N-S neotectonic basin, known as the Polis graben (Robertson, 1977b), while Pleistocene non-marine sediments occur near the coast (Balmer *et al.*, 2019) (see Fig. 2).

Based on structural and sedimentary studies (Elion, 1983; Payne & Robertson, 1995, 2000; Kinnaird & Roberson, 2013), the Polis graben has been interpreted as a rift basin that mainly formed during the Mid-Late Miocene, with extension continuing into Pliocene and Pleistocene. The rift is inferred to have developed above a subduction zone that, in this area, generally dipped eastwards, related to late-stage contraction of the Southern Neotethys. Structural work indicates that pervasive, rectilinear high-angle extensional faulting characterises the rift flanks (Payne & Robertson, 1995, 2000) and extends eastwards across the periphery of the Troodos ophiolite and its sedimentary cover (Chen & Robertson, 2018; their supplementary material). Recently, an alternative model has been proposed in which the

Polis graben is interpreted as a piggy-back basin above blind thrusts (Papadimitriou *et al.*, 2018). Deep well and/or seismic reflection data would be needed to test this model. The long-standing interpretation of the Polis graben as a Neogene extensional basin is, however, retained here**.**

The Miocene reefs and related facies in SE Cyprus (Fig. 2) are developed on a relatively elevated platform (Follows *et al.,* 1996), which largely conceals their relationship to the Miocene succession as a whole. In contrast, in NW Cyprus, both the Early and the Late Miocene reefs and related facies can be stratigraphically linked to the development of deeper-water facies within the Polis graben (Fig. 2). Dating of these deeper-water facies can, therefore, shed light on the timing of reef growth and demise (Cannings, 2018).

The Miocene deposits of the circum-Troodos succession, including the Polis graben, are traditionally mapped as the Pakhna Formation (Henson *et al.,* 1949; Constantinou, 1995). The contact between the Maastrichtian-Paleogene Lefkara Formation and the Neogene Pakhna Formation is inferred to be diachronous, both in S Cyprus (Eaton & Robertson, 1993) and W Cyprus (Banner *et al.,* 1999; BouDagher-Fadel & Lord, 2006). The Miocene Pakhna Formation in W Cyprus, as elsewhere, is dominated by hemipelagic carbonates and redeposited neritic carbonates. The Early Miocene Terra Member, as defined here, is constituted of very localised exposures of *in situ* reefs, together with more widespread exposures of related, redeposited facies. The Late Miocene Koronia Member is made up of locally developed *in situ* patch reefs, together with large volumes of redeposited, neritic-derived carbonates. The remainder of the Miocene succession is here termed, Pakhna Formation (undifferentiated).

In W Cyprus, the Early Miocene phase of reef development has been dated, generally as Burdigalian, mainly based on benthic foraminifera from associated carbonate facies (Follows *et al.,* 1996). The Early Miocene reefs were inferred to have formed prior to a phase of extensional faulting that initiated the Polis graben (Payne & Robertson, 1995, 2000). The Late Miocene phase of reef development was dated, generally as Tortonian, again mainly based on associated benthic foraminifera (Follows *et al.*, 1996). This later phase of reef development was interpreted as being coeval with the main phase of extensional faulting that created the Polis graben (i.e. syn-rift facies) (Payne & Robertson, 1995, 2000; Kinnaird & Robertson, 2013).

Previous dating

All of the available Sr isotope and biostratigraphic dates come from associated facies rather than from the reef frameworks and thus the ages of the reefs are inferred indirectly.

In SE Cyprus, benthic foraminiferal biostratigraphy, supported by some planktic foraminiferal and calcareous nannofossil biostratigraphy of spot samples, has indicated an Aquitanian-Burdigalian age for the Terra Member, near Cape Greco (Follows, 1992; Follows *et al.,* 1996). A small number of samples from the Terra Member in NW Cyprus suggested a similar age range, based on calcareous nannofossil biostratigraphy (Follows *et al.,* 1996). Benthic foraminiferal assemblages, together with some planktic foraminiferal assemblages, have been identified from seven sections in NW Cyprus, five of which are in our study area (Drousha-Kritou Terra, Kinousa, Kritou Terra, Pano Arodes and Terra sections), and ages were determined ranging from Aquitanian to Late Burdigalian (Banner *et al.,* 1999). An Aquitanian-Burdigalian age for the Terra Member was later confirmed using additional sections in the Akamas Peninsula, to the south of our study area (BouDagher-Fadel & Lord, 2006). Recently, *Sphenolithus heteromorphus*, *Helicosphaera ampliaperta*, and *H. scissura* were identified in calcirudites in the Pegeia area of W Cyprus, suggesting correlation of this outcrop with the Early Miocene Terra Member (Papadimitriou *et al.,* 2018). In addition, benthic foraminifera have been used to indicate a Late Miocene age for the Koronia Member in both SE and NW Cyprus (Follows, 1992; Follows *et al.*, 1996). In particular, *Borelis sp*. was noted in the Koronia Member (Follows *et al.*, 1996) and was taken to support a Late Miocene age (Follows, 1992; Follows *et al.*, 1996).

Methods

Reconnaissance geological mapping

To provide a framework for our new dating results, the existing geological maps of NW Cyprus were utilised and, where appropriate, revised. Our main resources were the 1: 250,000 Geological Map of Cyprus (Constantinou, 1995), a recent geological map of the Pliocene-Pleistocene in the northern Polis graben (Balmer *et al.*, 2019), and our own reconnaissance fieldwork. As a result, several new outcrops of Miocene-aged sediments were recognised and some existing outcrops and their stratigraphical contacts were re-assigned, mainly to the Pliocene (Fig. 3).

Sedimentary logging

To support our new dating, several well-exposed successions of the Pakhna Formation, representing both relatively proximal and more distal facies relative to the reefs, were selected and logged in detail (Fig. 6, logs 1-5). Representative samples were collected, mainly for age determination. We focused on sections in which pelagic facies (chalk) or hemipelagic facies (marl; i.e. calcareous mudstone containing clay and/or silt) are intercalated with redeposited facies, of potentially Terra Member or Koronia Member material.

Dating

Calcareous nannofossils

Thirty samples from the Pakhna Formation were studied, mainly to refine the ages of the hemipelagic background sediments throughout the northern Polis graben area (Fig. 5) (see Supplementary Material for GPS locations). The calcareous nannofossils were identified using smear slides prepared using the standard smear method (Backman & Shackleton, 1983; Henderiks & Törner, 2006), and then examined with a light microscope at a magnification of x1000-1250. The calcareous nannofossil biostratigraphy is based on Backman *et al.* (2012) (see Table S2).

Benthic foraminifera

Benthic foraminifera were examined from two localities in the northwest of the Polis graben (Fig. 5), both as individual specimens and in orientated thin sections. Samples were soaked in water, then washed through a 32 μm sieve and dried. For orientated thin sections, individual specimens were separated from the host rock, mounted in epoxy resin and abraded with silicon carbide in order to expose the equatorial layer and the embryonic apparatus. The specimens were then fixed to a standard thin section slide using UV-sensitive Loctite glue;

excess material was removed by polishing. The resulting thin sections were observed using a polarising transmitted light microscope (at 120x and 400x magnification). Identification of the mounted specimen was based on the biometric parameter of the embryo, following the taxonomy proposed by Özcan & Less (2009) and Özcan *et al.* (2010). The results were compared to the biozones of Cahuzac & Poignat (1997).

Planktic foraminifera

Sixty samples of planktic foraminifera from selected locations (localities are listed in Supplementary Material, Table S3) were soaked in water for 24 hours and then washed over a 63 μm sieve in order to remove clay and silt grain matrix. Foraminiferal residues were dry-sieved using 150 μm, 250 μm and 355 μm-sized sieves and split into aliquots of ≈200 specimens per size fraction. The biostratigraphy utilises the biozones of Wade *et al.* (2011) and the stratigraphy of both Iaccarino *et al.* (2011) and Lirer *et al.* (2019).

Strontium isotopes

Planktic foraminifera were picked from 19 samples of undifferentiated Pakhna Formation, and also from marl horizons associated with reef deposits throughout the northern Polis graben (Fig. 5) (see Supplementary Material for GPS locations). The isotopic analysis was carried out using a VG-Sector-54 thermal ionization mass spectrometer in order to establish $^{87}Sr/^{86}Sr$ ratios. Strontium isotopic ages were calculated using the LOWESS Sr isotope Look-Up Table (Version 4: 08/04) (McArthur *et al.,* 2001; McArthur & Howarth, 2004). The total combined errors were calculated from a combination of empirical instrumental errors, the analytical errors and the errors resulting from the LOWESS Sr curve (McCay *et al*. 2013; see Supplementary Material).

Results

Stratigraphy

The reconnaissance geological mapping (Fig. 3), supported by the new age data (see below), allows four facies of the Pakhna Formation to be distinguished. The first facies is redeposited sediments, correlated with the Early Miocene Terra Member (in situ reefs are minimal; see below). The second is redeposited sediments of the Koronia Member of Mid-Late Miocene age, the third is *in situ* reefs of the Koronia Member also of Mid-Late Miocene age and the fourth is undifferentiated Pakhna Formation, mostly marl and chalk.

The Miocene successions in NW Cyprus differ on both flanks and in the depocentre of the Polis graben (Fig. 6). All of the units of the Pakhna Formation are exposed on the west flank of the graben (although not as a continuous succession), whereas only undifferentiated Pakhna Formation and the Koronia Member are exposed on the eastern flank. The intervening basin depocentre is restricted to the undifferentiated Pakhna Formation. A representative E-W cross-section of the Polis graben (modified from Payne & Robertson, 1995) (Fig. 7) shows that the outcrops of the reefs and related facies are structurally controlled. In particular, the Terra and Koronia members are exposed in different fault blocks on the western flank of the graben.

In NW Cyprus, the Terra Member reef facies was only found exposed *in situ* in one very small area on the upper NW flank of the graben, near Androlikou (Figs. 3, 8E). This exposure, numerous reworked reef blocks in the vicinity, and associated talus deposits have a relatively high biodiversity of corals, including *Tarbellastraea*, *Porites* and *Favia* (Follows *et al.*, 1996). The Terra Member as a whole is dominated by reef-derived talus, mostly debris flow-deposits, as well exposed on the upper eastern slopes of the Akamas Peninsula in the key Kourroulla Gorge section (named after the stream course at the northern end of the gorge) (Fig. 3).

In NW Cyprus, *in situ* reef and closely related facies of the Koronia Member are exposed on the western flank of the graben, represented by circular to elongate exposures, typically up to 100s of m long and up to *c.*, 20 m thick, mainly located near the crest of the northern Akamas Peninsula (Fig. 3). The Koronia Member is also widely distributed, mainly as redeposited material, along the upper, eastern slopes of the graben, typically as elongate depositional units, up to *c.* 7 km long by 30 m thick (e.g. near Pelathousa) (Fig. 3).

The Koronia Member reef is dominated by poritid corals (Fig. 8F) which are often poorly preserved, associated with calcareous algae, benthic foraminifera, serpulids, echinoids and other neritic fauna (Follows *et al.*, 1996). Locally (e.g. near Steni) (Fig. 3), on the NE graben flank, the upper surface of the reefal material is karstified and dissected by neptunian fissures that are locally infilled with marl (Fig. 8G), which was dated as Pliocene (see below). Pliocene marl deposits stratigraphically overlie the neptunian fissures on the NE graben flank. Many of these high-elevation Pliocene deposits on the east flank are cut by high-angle extensional faults (orientated approximately NNE-SSW).

Sedimentology

A continuous vertical succession is very well exposed in Kourroulla Gorge, NW Akamas Peninsula (Figs. 3; 7, log 1), This begins with matrix-supported conglomerates (calcirudites), interpreted as debris-flow deposits; these contain abundant clasts of benthic foraminiferal packstone/grainstone, rhodoliths and reworked reef material. The clasts within the matrix-supported conglomerate are interpreted to have been derived from the Terra Member, based on their composition, including several types of coral characteristic of the Terra Member reefs (*Tarbellastraea*, *Porites* and *Favia).* Overlying well-bedded marl, normal-graded calcarenites and matrix-supported conglomerates (calcirudites) contain contrasting material typical of the Koronia Member, including poritid coral and calcareous algae. Assuming these stratigraphic correlations are correct, dating of the relatively fine-grained marl between the Terra versus Koronia member-derived material could indicate when Terra Member reef development ended and Koronia Member reef development started, and also the time that elapsed between these two events.

Two shorter successions that were measured on the eastern flank of the graben (Pano Akouradelia sections A & B) (Fig. 4, logs 2 and 3) also contain coarse coral debris and could, therefore, help to date when carbonates (Terra Member and/Koronia Member) were redeposited from the adjacent reefs. An additional succession of fine-grained sediments that includes organic carbon-rich layers (potential sapropels) (Pano Akouradelia section C) (Fig. 4, log 4) was inferred to represent a relatively high (young) part of the Pakhna Formation and might, as a result, shed light on the final Late Miocene reef demise (Koronia Member), prior to the Messinian salinity crisis.

In addition, representative of the Miocene succession on the eastern flank of the graben, a long, intact section of redeposited carbonates was logged near Evretou Dam (Fig. 4, log 5). Based on its composition, including poritid coral debris, these deposits were previously correlated with the Koronia Member (Payne & Robertson, 1995; Constantinou, 1995).

Chronology

Calcareous nannofossils

Samples of redeposited sediments from the west flank of the graben that include Terra Member reef material contain Early to Middle Miocene nannofossils (Table S2). Samples taken from above (TC1787) and below (TC1786) the last calcirudite (debris flow) bed at the base of the section in Kouroulla Gorge (Fig. 8A, B, C, D, Fig. 4, log 1) are dated as 13.53-13.9 Ma (biozone CNM7) (based on the presence of *Sphenolithus heteromorphus*) (Fig. 9).

Samples from the east flank of the graben (TC1768, 80), previously mapped as Late Miocene Koronia Member (Payne & Robertson, 1995; Constantinou, 1995) were found to contain nannofossil assemblages of Pliocene age (biozones CNPL1-CNPL4) (5.36 Ma – 2.76 Ma) (Table S2), indicating that in this case the coral debris was reworked long after reef growth ended.

Benthic foraminifera

Three samples that contain abundant, well-preserved large benthic foraminifera (LBF) were studied from the west flank of the graben (Fig. 10). The most LBF-rich sample, from the central western flank of the graben (*c.* 2.5 km S of Neo Chorio) (TC1749), is characterized by *Nephrolepidina praemarginata*, *Nephrolepidina morgani*, *Eulepidina* sp. *Heterostegina* cf. *borneensis* and *Amphistegina* sp., together with probable *Operculina* sp., and also *Nummulites* sp. This assemblage, taking account of the absence of *Miogypsina* sp. and

Miogypsinoides sp, suggests an Early Chattian (Late Oligocene) age, and can be assigned to the Shallow Benthic Zone 22B of Cahuzac & Poignant (1997).

Two additional samples from the northern Akamas Peninsula (*c.* 2.5 km NW of Akamas) (TC1746 and TC1747) (Fig. 10) contain a different faunal assemblage, characterized by abundant miliolids, including the age-diagnostic species *Borelis melo melo*; while, large rotalids such as *Nephrolepidina* and *Myogypsina* are absent. The assemblage suggests a Middle to Late Miocene age; i.e. earliest Langhian, *c.* 16 Ma to Mid-Messinian, *c.* 6 Ma (Cahuzac & Poignant, 1997). The two samples also contain common *Dendritina* sp., which, together with *Borelis melo melo*, suggest a Late Miocene age (Betzler & Schmitz, 1997).

Planktic foraminifera

60 samples were studied (see supplementary material for sample locations and characteristic assemblages). Based on age-diagnostic species four distinct planktic foraminiferal assemblages can be identified, indicating specific time intervals: (1) A Middle Miocene assemblage characterised by *Orbulina universa, Globoquadrina spp, Paragloborotalia siakensis & Orbulina suturalis*; (2) A Late Miocene-Early Pliocene assemblage characterised by *Globorotalia margaritae, Sphaeroidinellopsis seminulina, Globoturborotalita nepenthes & Neogloboquadrina acostaensis*; (3) A Late Pliocene assemblage characterised by *O. universa, Globigerinoides ruber, Sphaeroidinella dehiscens & Globigerinoides extremus*; (4) An Early Pleistocene assemblage characterised by *O. universa, G. ruber & S. dehiscens* (see Supplementary Material Table S3). The foraminiferal ages are used to support the results from the other dating methods (rather than as a stand-alone technique) because of the absence

of many key age-diagnostic species in the Mediterranean and the relatively low temporal precision of planktic foraminifera biozones in the Miocene (Lirer *et al.*, 2019).

Strontium isotopes

New Sr isotope dates (19 samples) are summarised in Figure 11. For the Kouroulla Gorge section on the west flank of the graben (Fig. 4, log 1) an age of *c.* 9.3 Ma was obtained for a sample from near the top of the marl sequence (TC1792), directly beneath the coarse redeposited facies correlated with the Koronia Member. For the reference section on the eastern flank, near Evretou Dam (Fig. 4 log 5), a marl sample (TC17122) between beds of reef-derived material gave an age of *c.* 6.1 Ma, confirming correlation with the Koronia Member. In addition, samples (TC1705, 09, 10, 13 68, 69, 79) collected from exposures on the east flank of the graben yielded Pliocene and Pleistocene ages, supporting the remapping of these sections (Fig. 3). An Early Pliocene age (*c.* 5.2 Ma) was obtained for a sample of pink marl that infills the neptunian fissures on the karstified, uppermost surface of the limestone correlated with the Koronia Member (Fig. 8G).

Discussion

Chronology and palaeo-environments of deposition

Our new dating, when integrated with existing data, indicates a revised timing of reef and reef related facies development in NW Cyprus (Fig. 12).

Oligocene to Early Miocene

Assemblages of benthic foraminifera that are dominated by a diverse fauna of large rotalids, similar to the Early Chattian assemblage determined here, occur widely within shallow-water carbonates of Late Oligocene and Early Miocene age elsewhere in the Tethyan region (e.g. Matteucci & Schiavinotto, 1977; Bosellini *et al.*, 1987; Bosellini & Perrin, 1994; Özcan *et al.*, 2009; Tomassetti *et al.*, 2013; Pomar *et al.*, 2014; Coletti *et al.*, 2018, 2019). Our Early Chattian benthic foraminifera come from a localised (isolated) exposure (≈1 m across) near the crest of the Akamas Peninsula (Fig. 5). This is part of an outcrop that was previously included within foraminifera-rich calcarenites of the Terra Member (Follows *et al.*, 1996). The material is reworked within debris flow-deposits. Pelagic sediments of Oligocene age were previously identified in W Cyprus near Paphos (Fig. 2), directly SW of the Geroskipou exit of the A6 highway (BouDagher-Fadel & Lord, 2006). The presence of Late Oligocene benthic foraminifera, therefore, indicates the former existence of a shallow-water carbonate shelf (of unknown dimensions) near the present crest of the northern Akamas Peninsula.

Our Early to Middle Miocene ages of nannofossils from the western flank of the graben in Kouroulla Gorge (Table S2) are consistent with derivation from the Terra Member reefs that were previously dated as Aquitanian-Burdigalian in the Akamas Peninsula, using benthic and/or planktic foraminifera (Follows *et al.*, 1996; BouDagher-Fadel & Lord, 2006). The inferred Oligocene carbonate platform could have provided a suitably firm foundation for the Early Miocene reefs. Based mainly on the evidence of the coarse redeposited facies, one or more patch reefs, with diverse coral species, developed near the present crest of the NW Akamas Peninsula during the Early Miocene (Fig. 13A). The presence of clasts of benthic foraminiferal packstone/grainstone, rhodoliths (in additional to Terra Member corals) within the redeposited material (e.g. Kouroulla Gorge) (Figs. 3, 8B, C, D; 7, log 1) suggest that the patch reefs were fringed by rhodoliths and benthic foraminiferal shoals, as inferred in both

SE Cyprus (Follows, 1992) and NW Cyprus (Follows *et al.*, 1996). Additional neritic facies accumulated further south, including the Pegeia area. However, elsewhere in W Cyprus chalk and marl deposition (undifferentiated Pakhna Formation) persisted during the Early Miocene, indicating areas where water depths were too great or where the substratum was unsuitable for reef growth.

Middle Miocene

There is no facies or age evidence of continued reef development during the Middle Miocene anywhere in Cyprus. Along the NW flank of the Polis graben, debris flow-deposits were eroded from the pre-existing Early Miocene reefs and related facies (Terra Member) and accumulated within adjacent hemipelagic deposits, as exposed in Kouroulla Gorge (Fig. 8B, C, D, 7, log 1). Farther south in the Akamas Peninsula, at Pano Akourdalia and Pano Arodes (Fig. 4, logs 2, 3), marl samples (undifferentiated Pakhna Formation) gave Langhian-Serravalian ages (Table S2) corresponding to biozones mid CNM7- CNM8 (i.e. 14.86 Ma - 12.57 Ma). This suggests that the western flank of the Polis graben (at least the southern part) remained in relatively deep water during the Mid-Miocene. In addition, hemipelagic sedimentation (undifferentiated Pakhna Formation) continued near the basin depocentre (Figs. 4, 5), as is indicated by the Langhian (CNM7) age of sample TC17143 (hemipelagic marl), collected *c.* 2 km ESE of Androlikou.

Late Miocene

Most of our Koronia Member samples lack age-diagnostic microfossils or are unsuitable for dating because of recrystallisation. However, two samples from the west flank of the graben in the Akamas Peninsula (approximately north east of Akamas Village) (Fig. 10) (TC1746 and TC1747) contain Middle-Late Miocene benthic foraminiferal assemblages. A Late Miocene age is very likely for these samples due to the association of *Dendritina sp.* with *Borelis melo melo,* and thus confirms the mapping as part of the Koronia Member.

Some bioclastic calcarenites (packstones/grainstones) on the east flank of the graben (e.g. near Pelathousa) were previously mapped as the Early Miocene Terra Member based on apparent facies similarities (Payne & Robertson, 1995). However, one sample (TC17122) of calcareous mudstone from an interval located between bioclastic calcarenites and calcirudites (including coral reef talus) in the Evretou Dam section (Fig. 4, log 5) yielded calcareous nannofossils of Late Miocene age (biozones CNM11-CNM20). This sample was also dated at *c.* 6.1 Ma using Sr isotopes (Fig. 11), again confirming a correlation with the Koronia Member. Early Miocene neritic facies have not been confirmed along the eastern flank of the graben. The *c.* 6.1 Ma age also suggests that the Koronia Member reef development persisted into the earliest Messinian, longer than previously assumed (Follows *et al.*, 1996).

During the Late Miocene, patch reefs developed on both the western and eastern flanks of the Polis graben, dominated by a poritid corals, together with marginal benthic foraminifera and rhodolith-rich facies (Follows *et al.*, 1996) (Fig. 13B). Extensional faulting was highly active during the Late Miocene (Payne & Robertson, 1995). The resulting tilted and uplifted fault blocks were ideal for patch reef development, as along the northern margin of the Troodos Massif (Follows and Robertson 1990; Follows *et al.*, 1996). Debris flow-deposits and calciturbidites infilled the structurally-controlled sediment accommodation space surrounding the patch reefs, with more distal facies reaching the depocentre of the Polis graben (although this is mostly concealed by Pliocene sediments).

During the Messinian salinity crisis (Hsü *et al.*, 1973; Meilijson *et al.*, 2019), gypsum and related facies accumulated within a roughly circular depocentre in the south of the Polis graben (c. 20 km in diameter), known as the Polemi basin (Robertson, 1977a; Orszag-Sperber *et al.*, 1989, 2009; Manzi *et al.*, 2016). In contrast, the uplifted flanks of the graben were subaerially exposed and locally karstified, as observed locally on the east flank (e.g. SE of Pelathousa). Elsewhere, Miocene sediments were eroded to form small volumes of fluvial sediments (e.g. at Evretou Dam) (Robertson, 1998a; Kinnaird & Robertson, 2013).

Pliocene

Pinkish marl (TC1705 – *c.* 5.2 Ma) that locally infills neptunian fissures (Fig. 8G) in the erosional surface of the Koronia Member on the east flank of the Polis graben was dated as Pliocene using planktic foraminiferal and Sr isotope dating and can, therefore, be correlated with the Nicosia Formation (Fig. 6). The presence of neptunian fissures extending down beneath a karstified surface confirms that subaerial exposure took place during the Messinian salinity crisis.

In response to earliest Pliocene (Zanclean) re-flooding of the Mediterranean (Hsü *et al.*, 1973; Spezzaferri *et al.*, 1998; Iaccarino *et al.*, 1999; Spezzaferri & Tamburini, 2007), Pliocene marine marls with a rich neritic shelly fauna progressively covered the Messinian land surface. The karstified erosion surface on the Koronia Member (with neptunian fissures) was covered by *c.* 5.2 Ma. This timing suggests that deposition of the Nicosia Formation began on the NW flank of the graben *c.* 100 kyr earlier than previously envisaged (Balmer *et al.*, 2019). Deposition in the depocentre is likely to have begun slightly earlier than this.

Sediment burial proceeded generally from north to south, controlled by the overall graben topography. The depocentre became more elevated southwards, beginning in Chrysochou Bay to the NW of Polis, extending down the northern Polis graben, and across the former Polemi basin until it terminated southwards (Balmer *et al*., 2019). The northern graben depocentre shallowed during the Late Pliocene (*c.* 2.76 Ma), initiating shallower-water calcareous bioclastic sedimentation, which is correlated with the Athalassa Formation in its type area, near Nicosia (Balmer *et al*., 2019). The southern graben depocentre remains poorly documented, however, NW Cyprus emerged during the Pleistocene, together with the Troodos Massif and Cyprus as a whole (Kinnaird *et al*., 2011; Palamakumbura *et al*., 2016).

The distribution of sedimentary facies in relation to the mapped faults shows that crustal extension continued during the Pliocene and Pleistocene to Recent (Payne & Robertson, 1995; Kinnaird & Roberson, 2013; Balmer *et al*., 2019), contributing to the present topography of the Polis graben. The relatively high elevation of some of the newly discovered Pliocene exposures, especially on the east flank of the graben (i.e. sample TC1705 is currently at *c.* 150 m above sea level) suggests that extensive fault-controlled uplift continued well into the Pliocene and possibly later. This late-stage faulting is supported by the presence of numerous high-angle extensional faults (orientated NNW-SSE) cutting the Pliocene deposits.

Regional to global comparisons

Early Miocene reefs

The relatively large outcrop of the Terra Member near Cape Greco in SE Cyprus is broadly of the same age (Aquitanian-Burdigalian) as that in NW Cyprus (Fig. 2). Patch reefs, up to 80 m thick and 500 m in diameter (Follows, 1992), made up of hermatypic z-corals (i.e. symbiont-bearing sensu Bosellini & Perrin, 2008) developed on a tectonically stable platform, fringed by shoal facies that were dominated by large benthic foraminifera, calcareous red algae (rhodoliths) and echinoids (Follows, 1992).

In the western Mediterranean region, Early Miocene reefs and related facies, similar to those of the Terra Member, are reported from Sardinia and Corsica (e.g. Galloni *et al.,* 2001; Benisek *et al.,* 2009; Tomassetti *et al.,* 2013) (Fig. 1). The reefs in Corsica reach >1 km in diameter and up to 12 m thick, and those in Sardinia > 350 m in diameter and up to 40 m in thickness (Galloni *et al.*, 2001). As in Cyprus, the diverse coral assemblages of the reefs were fringed by carbonate shoals with coralline algae, echinoids and large benthic foraminifera (e.g. Galloni *et al.,* 2001; Benisek *et al.,* 2009; Tomassetti *et al.,* 2013). The Bonifacio Basin in SE Corsica is remarkably similar in facies to the Terra Member (Follows *et al.*, 1996; Tomassetti *et al.*, 2013; Brandano *et al.*, 2016). Similar Early Miocene carbonates also accumulated on the Eratosthenes Seamount (open ocean), south of Cyprus (Fig. 2, inset). The seamount is interpreted as a continental fragment that rifted from the North African-Arabia continental margin, related to the opening of the Southern Neotethys (Robertson, 1998a; Kempler, 1998). The successions on the crest and on the northern flank of the Eratosthenes Seamount were drilled during Ocean Drilling Project Leg 160 (Hole 966F) (Emeis *et al.*, 1996). The Miocene sediments on the seamount accumulated on a relatively stable platform. The Early Miocene, lower part of the succession is characterised by a diverse assemblage of large benthic foraminifera and echinoids, remarkably similar to the shoals surrounding the Early Miocene (Terra Member) patch reefs in SE Cyprus (Follows *et al.*, 1996) and on the

Eratosthenes Seamount south of Cyprus (Coletti *et al*., 2019). These Early Miocene carbonates are overlain by a Mid-Miocene succession, rich in coralline red algae, then by a Late Miocene coral-rich interval, and finally by lagoonal facies (Robertson, 1998b; Coletti *et al.*, 2019; Coletti & Basso 2020).

In the western Mediterranean region, close to major landmasses, z-corals mainly formed small oligospecific bioconstructions (<5 m thick), as in Central Italy (Brandano, 2003; Civitelli & Brandano, 2005). Similar small biogenic structures (characterised by high species diversity) are inferred from reworked material, as in Northern Italy (Chevalier, 1962; Bosellini & Perrin, 2008; Perrin & Bosellini, 2012) and in SW France (Oosterbaan, 1988). In the Eastern Mediterranean region, again relatively close to land, relatively large (*c.* 1 km in diameter by up to 100 m in thick) z-coral build-ups are known in the Mut Basin, Southern Turkey (Bassant *et al.*, 2005; Pomar *et al.*, 2012). These reefs are dominated by poritid corals (Bassant *et al.*, 2005) and become larger further away from the local sources of siliciclastic sediment (Pomar *et al.*, 2012: Fig. 5). Sparse corals are also reported from the Early Miocene of the Adana Basin (Gurbuz, 2015).

The Corsica, Sardinia, Cyprus and Eratosthenes Early Miocene carbonate systems all developed away from major sources of siliciclastic sediment. This suggests that continental run-off, represented by high siliciclastic input and high levels of nutrients (both supplied fluvially) could have been detrimental to the Early Miocene carbonate factories, especially those dominated by z-corals. On the other hand, some carbonate-secreting organisms, such as coralline algae and benthic foraminifera, are known to survive even in sites of near-continuous siliciclastic influx (Wilson & Lokier, 2002; Lokier *et al*., 2009). For example, small coral-algal builds-up developed in the Miocene Kaş basin, SW Turkey, which is interpreted as a foreland basin in front of advancing thrust sheets (Hayward *et al.*, 1996). In general, however, settings away from high siliciclastic (and nutrient) influx excess nutrients appear to have favoured Early Miocene reef development.

Middle Miocene reefs

There is no record of Middle Miocene coral reefs or related facies in Cyprus. However, Mid-Miocene reefs and related facies are known elsewhere in the Eastern Mediterranean, in Israel (Buchbinder *et al*., 1993) and in the Mut basin (southern Turkey) (Vescogni *et al*., 2014). Middle Miocene reef development was more common in the western Mediterranean region; e.g. in Hungary (Oosterbaan, 1990), Austria (Riegel & Piller, 2000), N Italy (Chevalier, 1962), Algeria (Belkebir *et al.*, 1994), France (Chevalier, 1962; Cahuzac and Chaix, 1996) and Spain (Calvet *et al.*, 1994; Braga *et al.*, 1996).

Late Miocene reefs

In its type area, Koronia Hill, and elsewhere along the northern margin of the Troodos Massif, the Koronia Member developed as patch reefs and related neritic facies on tilted fault blocks, up to 3 km long by 800 m wide (Follows & Robertson, 1990; Follows *et al.*, 1996). The Koronia Member is also exposed in southern Cyprus, at Happy Valley, as large (up to tens of m-sized) detached blocks within mega-debris flow deposits. These blocks are interpreted to have been derived from a bathymetric high to the south, within an area of *c.* 1.5 km^2 in the Akrotiri Peninsula (Fig. 2). This local high was created by regional compression which affected southern Cyprus during the Early Miocene (Robertson *et al.*, 1991; Eaton & Robertson, 1993). The reef material and related neritic facies accumulated on a small shallow-water carbonate platform, followed by downslope collapse and reworking (probably tectonically triggered). In addition, the presence of redeposited reef talus (poritid corals) and reef-proximal facies (e.g. benthic foraminifera and red algae) within the Pakhna Formation, around the southern periphery of the Troodos massif (e.g. near Tokhni), points to the existence of Late Miocene fringing reefs that were later completely eroded (Robertson l977a; Eaton & Robertson, 1993).

In addition to *in situ* patch reefs, the Koronia Member includes abundant proximal, redeposited gravity-flow facies, as exposed in the Polis graben, along the north flank of the Troodos Massif (e.g. at Kottaphi Hill), at Happy Valley (S Cyprus) and along the southern periphery of the Troodos massif (e.g. at Tokhni). Similarly, the Tortonian-Messinian Pattish Formation, central Israel, is dominated by talus deposits that were derived from a *Porites*-dominated shelf-edge reef that is no longer preserved (Buchbinder *et al.*, 1993; Buchbinder & Zilberman, 1997).

The skeletal assemblage of the Koronia Member reefs is dominated by a monogeneric poritid-dominated assemblage (Follows, 1992). Similar Late Miocene assemblages characterise other depositional settings away from major land-masses, including the Eratosthenes Seamount (Robertson, 1998b; Coletti *et al.*, 2019; Coletti & Basso, 2020), the Salento Peninsula in southern Italy (e.g Bosellini *et al*., 2001; Bosellini *et al.*, 2002; Bosellini, 2006; Vescogni *et al.*, 2008), and the islands of Lampedusa (Grasso & Pedley, 1985) and Majorca (Pomar *et al.*, 1996). Comparable reefs also developed in near-continent settings, including Tuscany (Bossio *et al.*, 1996), Apulia (Bosellini *et al*., 2001; Bosellini *et al.*, 2002) and southern Spain (Esteban, 1996; Mankiewickz, 1996; Braga *et al.*, 2009). These poritid reefs also developed in a range of tectonically stable and unstable areas suggesting that they were able to cope with a wide range of sedimentary settings (Esteban, 1979).

Controls of reef growth and demise in NW Cyprus

We now attempt to assess the possible controls of reef development that could be applicable to northwest Cyprus, including sea-level rise or fall (local, regional or global), sea-water temperature/climate, nutrients, salinity and tectonic instability.

The Early Miocene reefs

An overall warm climate appears to have favoured the northward latitudinal expansion of z-corals during the Early Miocene-Langhian throughout the Mediterranean (Perrin & Bosellini, 2012). Ocean temperatures rose globally during much of the Early Miocene, peaking during the Mid-Miocene Climatic Optimum (*c*. 17–14.50 Ma; Burdigalian-Langhian) (Zachos *et al.,* 2001; Zachos *et al.*, 2008; De Vleeschouwer *et al.*, 2017; Miller *et al.,* 2020). Water temperatures then generally decreased, corresponding to the growth of the East Antarctic Ice Sheet (*c.* 13.7 Ma; late Serravallian) (Kennet *et al.,* 1975; Flower & Kennett, 1994; Holbourn *et al.,* 2005; Miller *et al.,* 2005). Although Mid-Miocene reefs are absent in Cyprus, the Serravallian drop in temperature, appears to have damaged coral reefs across the Mediterranean region, as indicated by a decrease in relative abundance, size and diversity during this time (Zachos *et al.*, 2001; Bosellini & Perrin, 2008; Perrin & Bosellini, 2012; Prista *et al.*, 2015).

Taxonomic coral richness decreases after the Burdigalian in line with decreasing temperatures in the Mediterranean region. Surprisingly, the Mid-Miocene Climatic Optimum is not obviously recorded in z-coral generic richness (Bosellini & Perrin, 2008), suggesting that temperature was not the sole control. Other possible controls include siliciclastic and nutrient run-off (Mutti *et al.*, 1997; Brandano *et al.*, 2017). During the Early-Middle Miocene, the Southern Neotethys between Arabia (North African plate) and the Taurides (Eurasian plate) effectively closed (Aktaş & Robertson, 1984; Ylmaz, 1993; Rögl, 1999; Hüsing *et al.*, 2009; Taylforth *et al.*, 2014). The collision was associated with very high siliciclastic (and potentially nutrient) supply, as documented in SE Turkey (Lice Formation) (e.g. Robertson *et al.*, 2016). Also, palaeoceanography (e.g. current systems) fundamentally changed as water exchange between the Mediterranean and the Indo-Pacific was curtailed. As a result, conditions may have become less favourable condition for z-corals.

Global (eustatic) sea-level change is another possible trigger of reef growth or demise. Sea-level highstands have been suggested to trigger high carbonate production as reefs attempt to keep up with rising sea-level (Schlager *et al.*, 1994; Schlager, 1999). However, the scope for greatly increased upward carbonate growth is limited for small patch reefs, unlike large carbonate platforms. Conversely, the absence of Mid-Miocene reefs in Cyprus (and elsewhere) might represent coral growth not keeping up with eustatic sea-level rise or rapid fluctuations (Robertson *et al.*, 1991). Modern reefs are generally capable of keeping pace with eustatic sea-level changes, especially small ones (e.g. Toscano & Macintyre, 2003; Toomey *et al.*, 2013).

The last (dated) debris-flow of Terra Member reef-derived material (13.53-13.9 Ma; Serravallian-Langhian boundary) (Fig. 14). This deposition (Fig. 8B, C, D; 7, log 1), was broadly contemporaneous with an isotopically-determined fall in global sea level of 50-60 m (Miller *et al.,* 2005; John *et al.,* 2011; Miller *et al.,* 2020), which corresponded to the *c.* 13.7 Ma growth of the East Antarctic Ice Sheet (Kennet *et al.,* 1975; Flower & Kennett, 1994; Holbourn *et al.,* 2005; Miller *et al.,* 2005).

Assuming the debris was derived directly from living reefs, then the end of the debris-flow deposition could be interpreted as the demise of the reef; i.e. at *c.* 13.7 Ma. A sudden sea-level fall could have exposed and killed off the reefs that were later eroded and reworked downslope as talus (although as noted above modern reefs typically adapts to sea-level change). However, it is very probable that the reefs died out earlier, around the Burdigalian-Langhian boundary (*c.* 16 Ma), such that the inferred sea level/temperature fall at *c.* 13.7 Ma only resulted in the reworking of dead coral and related talus. There are hints that this may be the case. The debris includes consolidated marl and chalk (Miocene and older) suggesting that this material is a second-cycle erosive product rather than having been shed directly from living reefs. Only the end of debris-flow deposition was dated at *c.* 13.7 Ma, whereas underlying debris-flows could be older and relate to previous sea-level falls or tectonic effects. Also, carbonate platform low-stand detritus, as documented elsewhere, is mainly thin, channelized lithic breccias with erosional debris that was derived from the by-then subaerially exposed reefs, as seen in the Late Eocene-Oligocene Maiella carbonate platform, Italy (Vecsei & Sanders, 1997). This contrasts with the relatively thick, lenticular and heterogeneous Mid-Miocene debris-flows in NW Cyprus. More dating of clasts in the other debris flows would help to test the alternatives.

Regional-scale tectonics are also known to have strongly influenced carbonate platforms during the Cenozoic (Bosence, 2005). The Langhian was characterised by tectonically-controlled deepening and marine transgression throughout many parts of the eastern Mediterranean region, including southern Turkey, namely the Köprü Basin (Flecker *et al.,* 2005), the Manavgat Basin (Flecker *et al.,* 1995), the Mut Basin (Şafak *et al.,* 2005), and the Adana Basin (Gurbuz, 1999; Gurbuz, 2015), and the Hatay Basin, northern Syria (Hardenberg & Robertson, 2007). On the Eratosthenes Seamount a Mid-Miocene sea-level rise (not fall) has been inferred, related to a switch from the Early Miocene diverse large benthic foraminiferal and echinoid assemblage, to the Mid-Miocene faunally impoverished coralline red algal assemblages (Coletti *et al.,* 2019). Supporting evidence includes: 1. A decrease in shallow-water bioclasts including corals, thick-shelled large benthic foraminifera (e.g. *Amphistegina)*; 2. An increase in planktic foraminifera and deep-photic-zone benthic foraminifera (e.g. thin-shelled *Heterostegina*); 3. A shift from shallow water to relatively deep-water coralline algae (Coletti *et al.,* 2019; Coletti & Basso, 2020). The overall driver of the inferred tectonic subsidence, including the Eratosthenes Seamount, was the convergence of the African and Eurasian plates that led to rapid flexural subsidence (e.g. Robertson, 1990; Coletti *et al.,* 2019).

Local-scale tectonics could also play a role in the reef demise. The Early Miocene Terra Member carbonate platform developed on a high, representing a precursor to the modern Akamas Penisula (Fig. 13A). Reef development appears to have preceded the main phase of rifting of the Polis graben (Payne & Robertson, 1995; Follows *et al.,* 1996). However, when exactly the rifting began remains uncertain. Initial rifting could have destabilised the reefs and triggered the mass-wasting of talus, including the Mid-Miocene debris flow-deposits, as seen on the NW flank of the Polis graben in Kouroulla Gorge (Fig. 8B, C, D 7, log 1). These debris-flow deposits include clasts of benthic foraminiferal packstone/grainstone, reef debris, Pakhna Formation marl and older, Lefkara Formation chalk indicating relatively deep-level erosion that is likely to have resulted from tectonic uplift. The uppermost debris-flow deposits in the Kouroulla Gorge section (Fig. 4, log 1) continue to include Terra Member coral material. Marls above and below this redeposited unit contain Mid-Miocene (*c.* 13.53-13.9 Ma; Serravallian) (Table S2) calcareous nannofossils indicating that reef material continued to be redeposited until *c.* 13.7 Ma, although, as noted above, this may well have post-dated the death of the reefs. In any case, local tectonics are unlikely to have controlled the demise of the Early Miocene reefs because the reefs in SE Cyprus developed (and remained) or a relatively stable platform.

In summary, no single cause convincingly explains the end of Early Miocene (*c.* 16 Ma) reef development in Cyprus and some other areas of the Mediterranean. Instead, the individual reefs in different areas are likely to have experienced different combinations of controls; i.e. glacio-eustatic global sea-level/temperature fall, variable siliciclastic/nutrient input, changed current strength/distribution, regional tectonic subsidence, and local tectonic uplift/subsidence. In other words, around the end of the Burdigalian, the reefs in Cyprus and in many other areas seem to have faced a ‘perfect storm’ that they did not survive.

The Late Miocene reefs

Our Sr isotope dating suggests that the Koronia Member reef-phase in NW Cyprus started after 9.3 Ma (mid-Tortonian). In NW Cyprus, the reefs moved to a higher structural level on the graben flanks, following extensional subsidence of the depocentre. The timing corresponds to the end of the period of high precipitation and temperature in the Eastern Mediterranean (‘Tortonian wash-house’). (Prista *et al.,* 2015; Böhme *et al.,* 2008; Böhme *et al.,* 2011). The implied transition to a more arid climate resulted in reduced continental run-off and nutrient input, factors which could have helped trigger renewed reef growth (Hallock & Schlager, 1986; Fabricius, 2005).

Decreased seawater temperature during the Late Miocene is likely to have influenced the marked reduction in coral diversity compared to the Early Miocene (Zachos *et al.,* 2001, 2008; Holbourn *et al.,* 2005; Bosellini & Perrin, 2008). Based on their widespread occurrence in the Mediterranean in different local environmental settings, the *poritid*-dominated assemblages that characterise the Late Miocene reefs were probably relative resistant to environmental stresses such as decreased temperature, nutrients or salinity fluctuations (Pomar *et al.*, 2017). The effective exclusion of other coral taxa, in contrast to the Early Miocene reefs, *could have* favoured the rapid construction of the very large monogeneric poritid reefs (e.g. as in S Spain and Majorca). The Late Miocene z-corals in the Mediterranean had a high frame-building capacity, despite their diversity being very low (i.e. poritid-dominated Koronia Member reefs) (Bosellini & Perrin, 2008; Perrin & Bosellini, 2012; Vertino *et al*., 2014; Pomar *et al*., 2017). This diversity decrease is believed to relate to a combination of closure of the S. Neotethys-Indian Ocean gateway, the effects of slow northward migration of the Mediterranean region, and continuing global temperature decrease (Bosellini & Perrin, 2008; Vertino *et al*., 2014). In Cyprus and several other areas (e.g. S Italy, Bosellini *et al*., 2001; Bosellini *et al.*, 2002 & Majorca, Pomar *et al*., 1996) the poritid-dominated reefs were able to survive into the Early Messinian, as suggested by our 6.1 Ma Sr isotopic age.

Late Miocene reef growth was controlled less by environmental factors (e.g. temperature; water purity) than by the presence of a suitable substratum and water depth. Rifting of the Polis graben in NW Cyprus produced topographies and water depths eminently suitable for patch reef growth. Our dating of reef talus points to reef growth during late Mid-Miocene (Late Serravallian) (*c.* 9.3 Ma) to mid-Late Miocene (Mid-Messinian) (*c.* 6.1 Ma). Uplifted crust also provided suitable substrates for Late Miocene reef growth in the type area of the Koronia Member along the northern margin of the Troodos ophiolite (Follows & Robertson, 1990) and elsewhere, including the source platform of the Happy Valley material, and the southern periphery of the Troodos massif.

During the Messinian, the climate in the Eastern Mediterranean further deteriorated and was influenced by increased aridity across sub-tropical regions (Tzanova *et* al., 2015; Herbert *et al*. 2016). The uplift of the Himalayan mountain belt, and possible related changes to the South Asian Monsoon, together with the closure of the Paratethys Seaway could have contributed to increased aridity in the Eastern Mediterranean region (Tzanova *et* al., 2015; Herbert *et al*., 2016), although the intensity of aridification in this region is uncertain (Polissar *et al*. 2019).

However, such factors, alone are unlikely to explain the final demise of the Koronia Member reef phase. Instead, the main driver was the isolation of the Mediterranean from the Atlantic and the resulting dramatic sea level fall during the Late Messinian (40-50m fall at the Gibraltar Strait *c.* 5.6Ma, Ohneiser *et al*. 2015), including around Cyprus (Hsü *et al*., 1973; Robertson *et al.,* 1995; Krijgsman *et al.,* 2002; Duggen *et al.,* 2003; Kouwenhoven *et al.,* 2006; Roveri *et al.,* 2014; Manzi *et al.,* 2016; Meilijson *et al.,* 2019). Increased salinity associated with the sea-level fall is inferred to have affected marginal settings first, as in southern Turkey (Flecker *et al.,* 1998), and is likely to have finally terminated the Late Miocene Koronia Member reef development.

Conclusions

Benthic foraminiferal facies accumulated on a bathymetric high in the Akamas Peninsula, NW Cyprus, during Late Oligocene (Chattian) (27.8 – 23.0 Ma). The benthic foraminiferal assemblage is similar to shallow-water carbonates of Late Oligocene-Early Miocene age in some other areas of the Mediterranean region. The localised neritic facies in NW Cyprus contrast with continuing pelagic carbonate deposition elsewhere in southern Cyprus.

The Early Miocene Terra Member (Pakhna Formation) in NW Cyprus, as in SE Cyprus, was characterised by a diverse coral assemblage, with marginal facies including benthic foraminiferal shoals. The reefs in NW Cyprus are now almost entirely preserved as redeposited talus. Debris was shed from the Early Miocene reefs (along with associated and pre-existing facies) during the Mid-Miocene until *c.* 13.7 Ma (Serravallian). This detritus probably post-dates the reef growth. No one factor appears to have caused Early Miocene reef demise in NW Cyprus and many other areas of the Mediterranean. Controlling factors are likely to have included glacio-eustatic global sea-level/temperature fall, variable siliciclastic/nutrient input, changed current strength/distribution, regional tectonic subsidence, and local tectonic uplift/subsidence.

The second-phase, Koronia Member in NW Cyprus reef developed on structurally controlled highs, during rifting of the neotectonic Polis graben. Dating of talus supports major rifting during the Tortonian (*c.* 9.3 Ma) to mid-Messinian) (*c.* 6.1 Ma). Extensional tectonics persisted during the late-Messinian, Pliocene and Recent, based on sedimentary and structural evidence.

Reduced sea-water temperature, increased aridity and/or reduced siliciclastic input after the mid-Miocene are likely to have contributed to the nucleation and growth of environmentally resistant, monogeneric poritid corals during the Tortonian-early Messinian, as supported by new dating.

Acknowledgements

This paper stems from fieldwork and dating studies carried out for a Masters by Research thesis by the first author at the University of Edinburgh, and also takes account of on-going PhD research by the second author (Balmer) on the Late Cretaceous-Late Miocene sedimentary development of W Cyprus. We thank Anne Kelly and Vinnie Gallagher, Scottish Universities Environmental Research Centre, East Kilbride, for their assistance with the Sr isotopic analysis. The first author thanks Erin Alexander for her assistance during the initial fieldwork and Gillian McCay for scientific discussion and advice on figure preparation. We thank, Francesca Bosellini and one anonymous reviewer for constructive comments which improved this manuscript considerably.

Conflict of interest: The authors declare no known conflicts of interest associated with this paper.

References

Aktaş G. & Robertson A.H.F., 1984. The Maden Complex, SE Turkey: evolution of a Neotethyan active margin. *In*: Dixon J.E. & Robertson A.H.F. (eds) The Geological Evolution of the Eastern Mediterranean. Geological Society Special Publication, **17**, 375-402.

Backman, J. Raffi, I. Rio, D. Fornaciari, E. & Pälike, H., 2012. Biozonation and biochronology of Miocene through Pleistocene calcareous nannofossils from low and middle latitudes. *Newsletters on Stratigraphy*, **45,** 221-244.

Backman, J. & Shackleton, N.J., 1983. Quantitative biochronology of Pliocene and early Pleistocene calcareous nannofossils from the Atlantic, Indian and Pacific oceans. *Marine Micropaleontology*, **8**, 141–170.

Balmer, E. M. Robertson, A. H. F., Raffi, I. & Kroon, D., 2019. Pliocene–Pleistocene sedimentary development of the syntectonic Polis graben, NW Cyprus: Evidence from facies analysis, nannofossil biochronology and strontium isotope dating. *Geological Magazine*, **156,** 889–917.

Bagnall, P. S., 1960. The Geology and Mineral Resources of the Pano Lefkara-Larnaca area, Cyprus. Geological Survey Department Memoir, **5**, 116 p.

Banner, F. T., Lord, A. R. & BouDagher-Fadel, M. K., 1999. The Terra Limestones Member (Miocene) of Western Cyprus. *Greifswalder Geowissenschaftliche Beiträge*, **6**, 503-515.

Bassant, P., Van Buchem, F. S. P., Strasser, A. & Görür, N., 2005. The stratigraphic architecture and evolution of the Burdigalian carbonate-siliciclastic sedimentary systems of the Mut Basin, Turkey. Sedimentary Geology, **173**, 187-232.

Bear, L. M., 1960. The Geology and Mineral Resources of the Akaki-Lythrodondha area, Cyprus. Geological Survey Department Memoir**, 3**, 122 p.

Belkebir, L., Mansour, B., Bessedik, M., Saint-Martin, J.P., Belbarbi, M. & Chaix, C., 1994. Présence d'une construction récifale à Djebel Chott (Dahra occidental, Algérie): témoin du maximum transgressif du Miocène moyen en Méditerranée). *Interim Colloqu. RCMNS Marseille, France.(abstract book)*, **4**.

Benisek M-F., Betzler, C., Marcano, G. & Mutti, M., 2009. Coralline-algal assemblages of Burdigalian platform slope: implications for carbonate platform reconstruction (northern Sardinia, western Mediterranean). *Facies*, **55**, 375-386.

Betzler, *c.* & Schmitz, S., 1997. First record of Borelis melo and Dendritina sp. in the Messinian of SE Spain (Cabo de Gata, Province Almeria). *Palaeontologische Zeitschrift*, **71**, 211-216.

Bialik, O.M., Frank, M., Betzler, C., Zammit, R. & Waldmann, N.D., 2019. Two-step closure of the Miocene Indian Ocean Gateway to the Mediterranean. *Scientific Reports*, **9**, 8842, https://doi.org/10.1038/s41598-019-45308-7.

Böhme, M., Ilg, A. & Winklhofer, M., 2008. Late Miocene "washhouse" climate in Europe. *Earth and Planetary Science Letters*, **275**, 393–401.

Böhme, M., Winklhofer, M. & Ilg, A., 2011. Miocene precipitation in Europe: Temporal trends and spatial gradients. *Palaeogeography, Palaeoclimatology, Palaeoecology*, **304**, 212–218, https://doi.org/https://doi.org/10.1016/j.palaeo.2010.09.028.

Bosellini, F. R., 2006. Biotic changes and their control on Oligocene-Miocene reefs: A case study from the Apulia Platform margin (southern Italy). Palaeogeography, Palaeoclimatology, Palaeoecology, **241**, 393-409.

Bosellini A., Russo A., Arush M.A. & Cabdulquar M.M., 1987. The Oligo-Miocene of Eil (NE Somalia): a prograding coral-*Lepidocyclina* system. Journal of African Earth Sciences, **6**, 583-593.

Bosellini, F.R., Russo, A. & Vescogni, A. 2001. Messinian reef-building assemblages of the Salento Peninsula (southern Italy): palaeobathymetric and palaeoclimatic significance. *Palaeogeography, Palaeoclimatology, Palaeoecology*, **175**, 7–26, https://doi.org/https://doi.org/10.1016/S0031-0182(01)00383-2.

Bosellini, F.R., Russo, A. & Vescogni, A., 2002. The Messinian reef complex of the Salento Peninsula (southern Italy): Stratigraphy, facies and paleoenvironmental interpretation. Facies, **47**, 91–112.

Bosellini, F. & Perrin, C., 1994. The coral fauna of Vitigliano: qualitative and quantitative analysis in a back reef environment (Castro Limestone, Late Oligocene, Salento Peninsula, southern Italy). Bollettino della Società Paleontologica Italiana, **33**, 171-181.

Bosellini, F. R. & Perrin, C., 2008. Estimating Mediterranean Oligocene–Miocene sea-surface temperatures: an approach based on coral taxonomic richness. *Palaeogeography, Palaeoclimatology, Palaeoecology*, **258,** 71-88.

Bosence, D., 2005. A genetic classification of carbonate platforms based on their basinal and tectonic settings in the Cenozoic. *Sedimentary Geology,* **175**, 49-72.

Bossio, A., Esteban, M., Mazzanti, R., Mazzei, R. & Salvatorini, G., 1996. Rosignano reef complex (Messinian), Livornesi Mountains, Tuscany, Central Italy. Models for Carbonate Stratigraphy from Miocene Reef Complexes of Mediterranean Regions. *In:* Franseen E.K., Esteban M., Ward W.C. & Rouchy J.M. (eds) Models for Carbonate Stratigraphy, from Miocene Reef Complex of the Mediterranean Area. Concepts in Sedimentology and Paleontology, **5**, Society for Sedimentary Geology, Tulsa, Oklaoma, U.S.A, 277-294.

BouDagher-Fadel, M. & Lord, A., 2006. Illusory stratigraphy decoded by Oligocene-Miocene autochthonous and allochthonous foraminifera in the Terra Member, Pakhna Formation (Cyprus). *Stratigraphy*, **3**, 217-226.

Brachert, T. C., Betzler, C., Braga, J. *c.* & Martin, J. M., 1996. Record of climatic change in neritic carbonates: turnover in biogenic associations and depositional modes (Late Miocene, southern Spain). Geologische Rundschau, **85**, 327-337.

Brachert, T. C., Reuter, M., Kroeger, K. F. & Lough, J. M., 2006. Coral growth bands: a new and easy to use paleothermometer in paleoenvironment analysis and paleoceanography (late Miocene, Greece). Paleoceanography, 21(4). https://doi.org/10.1029/2006PA001288

Braga, J.C., Jimenez, A.P., Martin, J.M. & Rivas, P., 1996. Middle Miocene Coral-Oyster Reefs, Murchas, Granada, Southern Spain, *In:* Franseen E.K., Esteban M., Ward W.C. & Rouchy J.M. (eds) Models for Carbonate Stratigraphy, from Miocene Reef Complex of the Mediterranean Area. *Concepts in Sedimentology and Paleontology,* **5**, Society for Sedimentary Geology, Tulsa, Oklaoma, U.S.A, 131-139.

Braga, J. *c.* & Aguirre, J., 2001. Coralline algal assemblages in upper Neogene reef and temperate carbonates in Southern Spain. Palaeogeography, Palaeoclimatology, Palaeoecology, **175**, 27-41.

Braga, J.C., Vescogni, A., Bosellini, F.R. & Aguirre, J., 2009. Coralline algae (Corallinales, Rhodophyta) in the western and central Mediterranean Messinian reefs. *Palaeogeography Palaeoclimatology* Palaeoecology, **275**, 113-128.

Brandano M., 2003. Tropical/subtropical inner ramp facies in lower Miocene “Calcari a briozoi e litotamni” of the Monte Lungo area (Cassino Plain, Central Apennines, Italy). Bollettino Società Geologica Italiana, **122**, 85-98.

Brandano, M., Bosellini, F.R., Mazzucchi, A. & Tomassetti, L., 2016. Coral assemblages and bioconstructions adapted to the depositional dynamics of a mixed carbonate-siliciclastic setting: the case study of the Burdigalian Bonifacio Basin (South Corsica), *Rivista Italiana di Paleontologia e Stratigrafia*, **122**, 37-52.

Brandano, M., Cornacchia, I., Raffi, I., Tomassetti, L. & Agostini, S., 2017. The Monterey Event within the Central Mediterranean area: The shallow- water record. Sedimentology, **64,** 286-310.

Buchbinder, B. Martinotti, G. M. Siman-Tov, R. & Zilberman, E., 1993. Temporal and spatial relationships in Miocene reef carbonates in Israel. *Palaeogeography, Palaeoclimatology, Palaeoecology*, **101**, 97-116.

Buchbinder, B. & Zilberman, E. 1997. Sequence stratigraphy of Miocene-Pliocene carbonate-siliciclastic shelf deposits in the eastern Mediterranean margin (Israel): effects of eustasy and tectonics. *Sedimentary Geology*, **112**, 7–32.

Cahuzac, B. & Chaix, C., 1996. Structural and faunal evolution of Chattian–Miocene reefs and corals in western France and the northeastern Atlantic Ocean *In:* Franseen, E. K. Esteban, M. Ward, W. *c.* & Rouchy, J. (eds) *Models for Carbonate Stratigraphy from Miocene Reef Complexes of Mediterranean Regions,* Society of Economic Paleontologists and Mineralogists, Tulsa, Oklahoma, 105-127.

Cahuzac, B. & Poignant, A., 1997. Essai de biozonation de l’Oligo-Miocène dans les bassins européens à l’aide des grands foraminifères néritiques. *Bulletin de la Société géologique de France*, **168**, 155-169.

Calvet, F., Esteban, M. & Permanyer, A., 1994. Mid Miocene coral reefs in the Gulf of Valencia, NE Spain. *In*: Saint Martin, J.P. Cornee, J.J. (eds) *Miocene Reefs and Carbonate Platforms of the Mediterranean. Interim Colloquium RCMNS, Marseille*, 3–6.

Cannings, T., 2018. *Microfossil and strontium isotope constraints on the age and development of the Miocene-Pliocene Polis graben, North West Cyprus.* Masters thesis (unpublished), University of Edinburgh.

Civitelli, G., Brandano, M., 2005. Atlante delle litofacies e modello deposizionale dei Calcari a Briozoi e Litotamni nella Piattaforma carbonatica laziale-abruzzese. Bollettino Società Geologica Italiana, **124**, 611-643.

Chen, G. & Robertson, A. H. F., 2019. Provenance and magmatic-tectonic setting of Campanian-aged volcaniclastic sandstones of the Kannaviou Formation in western Cyprus: Evidence for a South-Neotethyan continental margin volcanic ar*c*. Sedimentary Geology, **388**, 114-138.

Cherchi, A., Murru, M. & Simone, L. 2000. Miocene carbonate factories in the syn-rift Sardinia Graben subbasins (Italy). *Facies*, **43,** 223–240, https://doi.org/10.1007/bf02536992.

Chevalier J.P., 1962. Récherches sur les madréporaires et les formations récifales miocènes de la Méditerranée occidentale. Mémoires de la Société Géologique de France, **93**, 1–558.

Cohen, K.M., Harper, D.A.T., Gibbard, P.L., 2020. ICS International Chronostratigraphic Chart, 2020/01. International Commission on Stratigraphy, IUGS. www.stratigraphy.org

Coletti, G., Stainbank, S., Fabbrini, A., Spezzaferri, S., Foubert, A., Kroon, D. & Betzler, C., 2018. Biostratigraphy of large benthic foraminifera from Hole U1468A (Maldives): A CT-scan taxonomic approach. *Swiss Journal of Geosciences*, **111**, 523-536.

Coletti, G., Basso, D., Betzler, C., Robertson, A.H.F., Bosio, G., El Kateb, A., Foubert, A., Meilijson, A., Spezzaferri, S., 2019. Environmental evolution and geological significance of the Miocene carbonates of the Eratosthenes Seamount (ODP Leg 160). *Palaeogeography Palaeoclimatology Palaeoecology***,** **530**, 217-235.

Coletti, G. & Basso, D., 2020. Coralline algae as depth indicators in the Miocene carbonates of the Eratosthenes Seamount (ODP Leg 160, Hole 966F). Geobios, **60,** 29-46.

Constantinou, G., 1995.*1: 100,000 Geological Map of Cyprus*. Geological Survey Department, Nicosia, Cyprus.

Danese, E., 1999. Upper Miocene carbonate ramp deposits from the southernmost part of Maiella Mountain (Abruzzo, Central Italy). *Facies*, **41**, 41–54.

De Vleeschouwer, D., Vahlenkamp, M., Crucifix, M. & Pälike, H., 2017. Alternating Southern and Northern Hemisphere climate response to astronomical forcing during the past 35 m.y. *Geology*, **45**, 375–378.

Duggen, S., Hoernle, K., Van den Bogaard, P., Rüpke, L. & Morgan, J. P., 2003. Deep roots of the Messinian salinity crisis. *Nature*, **422** (6932), 602-606.

Eaton, S. & Robertson, A. H. F., 1993. The Miocene Pakhna Formation, southern Cyprus and its relationship to the Neogene tectonic evolution of the Eastern Mediterranean. *Sedimentary Geology*, **86**, 273-296.

Elion, P., 1983. Etude structural et sédimentologique du bassin Neogène de Pissouri (Chypre). Thèse 3è cycle, Université de Paris Sud, Orsay, France.

Emeis K.C., Robertson A.H.F., Richter C., *et al*., 1996. Proceedings of the Ocean Drilling Program, Initial Reports, **160**, Ocean Drilling Program, College Station, Texas, U.S.A, 972p.

Esteban, M., 1979. Significance of the upper Miocene coral reefs of the western Mediterranean. *Palaeogeography, Palaeoclimatology, Palaeoecology*, **29**, 169-188.

Esteban, M., 1996. An overview of Miocene reefs from Mediterranean areas: general trends and facies models. *In:* Franseen, E. K. Esteban, M. Ward, W. *c.* & Rouchy, J. (eds) *Models for Carbonate Stratigraphy from Miocene Reef Complexes of Mediterranean Regions,* Society of Economic Paleontologists and Mineralogists, Tulsa, Oklahoma, 3-53.

Fabricius, K.E. 2005. Effects of terrestrial runoff on the ecology of corals and coral reefs: review and synthesis. *Marine Pollution Bulletin*, **50**, 125–146, https://doi.org/https://doi.org/10.1016/j.marpolbul.2004.11.028.

Flecker, R., Robertson, A.H.F., Poisson, A. & Muller, C., 1995. Facies and tectonic significance of two contrasting Miocene Basins in south coastal Turkey. *Terra Nova*, 7, 221–232.

Flecker, R., Ellam, R.M., Müller, C., Poisson, A., Robertson, A.H.F. & Turner, J., 1998. Application of Sr isotope stratigraphy and sedimentary analysis to the origin and evolution of the Neogene Basins in the Isparta Angle, southern Turkey. *Tectonophysics*, **298,** 83–101.

Flecker, R., Poisson, A. & Robertson, A.H.F., 2005. Facies and palaeogeographic evidence for the Miocene evolution of the Isparta Angle in its regional eastern Mediterranean context. *Sedimentary Geology*, **173**, 277–314.

Flower, B. P. & Kennett, J. P., 1994. The middle Miocene climatic transition: East Antarctic ice sheet development, deep ocean circulation and global carbon cycling. *Palaeogeography, Palaeoclimatology, Palaeoecology*, **108,** 537-555.

Follows, E. J., 1992. Patterns of reef sedimentation and diagenesis in the Miocene of Cyprus. *Sedimentary Geology*, **79,** 225-253.

Follows, E. J. & Robertson, A. H. F., 1990. Sedimentology and structural setting of Miocene reefal limestones in Cyprus. *In: Panayiotou A.* (ed) *Ophiolites: Oceanic Crustal Analogues.* Geological Survey Department, Nicosia, Cyprus, 207-216.

Follows, E. J. Robertson, A. H. F. & Scoffin, T. P., 1996. Tectonic controls on Miocene reefs and related carbonate facies in Cyprus. *In:* Franseen, E. K. Esteban, M. Ward, W. *c.* & Rouchy, J. (eds) *Models for Carbonate Stratigraphy from Miocene Reef Complexes of Mediterranean Regions,* Society of Economic Paleontologists and Mineralogists, Tulsa, Oklahoma, 295-315.

Franseen E.K., Esteban M., Ward, W.C., Rouchy, G.M., 1996. Models for carbonate stratigraphy from Miocene reef complexes of Mediterranean regions: introduction. *In:* Franseen, E. K. Esteban, M. Ward, W. *c.* & Rouchy, J. (eds) *Models for Carbonate Stratigraphy from Miocene Reef Complexes of Mediterranean Regions,* Society of Economic Paleontologists and Mineralogists, Tulsa, Oklahoma, V-IX.

Galloni, F., Cornee, J. J., Rebelle, M. & Ferrandini, M. (2001). Sedimentary anatomy of early Miocene coral reefs in South Corsica (France) and South Sardinia (Italy). *Géologie méditerranéenne*, **28**, 73-77.

Gass, I. G., 1960. The Geology and Mineral resources of the Dhali Area: Geological Survey Department Memoir, **4.**

Gass, I. G., Masson-Smith, E. M., 1963. The geology and gravity anomalies of the Troodos massif, Cyprus. Royal Society of London, Philosophical Transactions, Series A**, 255**, 417-467.

Grasso, M. & Pedley, H.M., 1985. The Pelagian Islands: a new geological interpretation from sedimentological and tectonic studies and its bearing on the evolution of the Central Mediterranean Sea (Pelagian Block). *Geologica Romana*, **24**, 13–34.

Gurbuz, K., 1999. Regional implications of structural and eustatic Controls in the evolution of submarine fans: an example from the Miocene Adana Basin, Southern Turkey. *Geological Magazine,* **136,** 311 – 319.

Gurbuz, M.O., 2015. Tectonic and sea level controls on the back-stepping early Miocene carbonate platforms: Adana Basin, Turkey. Masters thesis (unpublished), The University of Texas.

Hallock, P. & Schlager, W. 1986. Nutrient excess and the demise of coral reefs and carbonate platforms. *Palaios*, **1**, 389–398, https://doi.org/10.2307/3514476.

Hardenberg, M. F. & Robertson, A. H. F., 2007. Sedimentology of the NW margin of the Arabian plate and the SW–NE-trending Nahr El-Kabir half-graben in northern Syria during the latest Cretaceous and Cenozoic. *Sedimentary Geology*, 20**1**, 231–266.

Hayward, A. B., Robertson, A. H. F. & Scoffin, T. P., 1996. Miocene patch reefs from a Mediterranean marginal terrigenous setting in southwest Turkey. *In:* Franseen, E.K., Esteban M., Ward W.C.& Rouchy J.M. (eds) Models for Carbonate Stratigraphy from Miocene Reef complexes of the Mediterranean area. *Concepts in Sedimentology and Paleontology,* **5**, Society for Sedimentary Geology, Tulsa, Oklaoma, U.S.A, 317-332.

Henderiks, J. & Törner, A., 2006. Reproducibility of coccolith morphometry: Evaluation of spraying and smear slide preparation techniques. *Marine Micropaleontology,* **58**, 207–218.

Henson, F. R. S. Browne, R. V. & McGinty, J., 1949. A synopsis of the stratigraphy and geological history of Cyprus. *Quarterly Journal of the Geological Society*, **105,** 1-41.

Herold, N., Huber, M., Müller, R. D. & Seton, M., 2012. Modeling the Miocene climatic optimum: Ocean circulation. *Palaeoceanography and Palaeoclimatology*, **27,** doi:10.1029/2010PA002041

Herbert, T.D., Lawrence, K.T., Tzanova, A., Peterson, L.C., Caballero-Gill, R. & Kelly, C.S. 2016. Late Miocene global cooling and the rise of modern ecosystems. *Nature Geoscience*, **9**, 843–847, https://doi.org/10.1038/ngeo2813.

Hladil, J., Otava, J. & Galle, A., 1991. Oligocene carbonate buildups of the Sirt Basin, Libya. *In:* M.J. Salem, O.S. Hammuda, B.A. Eliagoubi (eds), *The Geology of Libya*, Symposium on the Geology of Libya, Elsevier, Amsterdam, **4**, 1401-1420.

Holbourn, A., Kuhnt, W., Schulz, M. & Erlenkeuser, H., 2005. Impacts of orbital forcing and atmospheric carbon dioxide on Miocene ice-sheet expansion. Nature, **438**(7067), 483-487.

Holbourn, A. E., Kuhnt, W., Clemens, S. *C.*, Kochhann, K. G., Jöhnck, J., Lübbers, J. & Andersen, N., 2018. Late Miocene climate cooling and intensification of southeast Asian winter monsoon. Nature communications, **9**, 1-13.

Hsü, K. J., Ryan, W. B. & Cita, M. B., 1973. Late Miocene desiccation of the Mediterranean. Nature, **242** (5395), 240-244.

Hüsing, S. K. Zachariasse, W. J. Van Hinsbergen, D. J. Krijgsman, W. Inceöz, M. Harzhauser, M. & Kroh, A., 2009. Oligocene–Miocene basin evolution in SE Anatolia, Turkey: constraints on the closure of the eastern Tethys gateway. *In:* Van Hinsbergen, D. J. J. Edwards, M. A. Govers, R. (eds) Collision and Collapse at the Africa-Arabia-Eurasia Subduction Zone, *Geological Society, London, Special Publications*, **311,** 107-132.

Iaccarino, S., Castradori, D., Cita, M. B., Di Stefano, E., Gaboardi, S., McKenzie, J. A. & Sprovieri, R., 1999. The Miocene/Pliocene boundary and the significance of the earliest Pliocene flooding in the Mediterranean. Memoire Società Geologica Italiana**, 54,** 109-131.

Iaccarino, S. M. Di Stefano, A. Foresi, L. M. Turco, E. Baldassini, N. Cascella, A. & Lirer, F., 2011. High-resolution integrated stratigraphy of the upper Burdigalian-lower Langhian in the Mediterranean: the Langhian historical stratotype and new candidate sections for defining its GSSP. *Stratigraphy*, **8,** 199-215.

Janson, X. Van Buchem, F. S. P. Dromart, G. Eichenseer, H. T. Dellamonica, X. Boichard, R. & Eberli, G., 2010. Architecture and facies differentiation within a Middle Miocene carbonate platform, Ermenek, Mut Basin, southern Turkey. *In:* Van Buchem, F. S. P. Gerdes, K. D. Esteban, M. (eds) Mesozoic and Cenozoic Carbonate Systems of the Mediterranean and the Middle East: Stratigraphic and Diagenetic Reference Models. *Geological Society, London, Special Publications*, **329**, 265-290.

John, C.M., Karner, G.D., Browning, E., Leckie, R.M., Mateo, Z., Carson, B. & Lowery, C., 2011. Timing and magnitude of Miocene eustasy derived from the mixed siliciclastic-carbonate stratigraphic record of the northeastern Australian margin. *Earth and Planetary Science Letters*, **304**, 455–467.

Kennett, J.P., Houtz, R.E., Shackleton, N.J. & Kennett, J.P., 1975. Paleotemperature History of the Cenozoic and the Initiation of Antarctic Glaciation: Oxygen and Carbon Isotope Analyses in DSDP Sites 277, 279 and 281. *In*: Kennett, J.P., Houtz, R.E., Shackleton, N.J. & Kennett, J.P. (eds) *Initial Reports of the Deep Sea Drilling Project*, U. S. Government Printing Office, **29**, 743–756.

Kempler, D., 1998. Eratosthenes Seamount: The Possible Spearhead of Incipient Continental Collision in the eastern Mediterranean. *In:* Robertson, A. H. F., Emeis, K.C., Richter, C. & Camerlenghi, A. (eds) *Proceedings of the Ocean Drilling Program, Scientific Results*, **160**, Ocean Drilling Program, College Station, TX, 709-721.

Kiessling, W., 2009. Geologic and biologic controls on the evolution of reefs. *Annual Review of Ecology, Evolution, and Systematics,* **40,** 173-192.

Kinnaird, T. C., Robertson, A. H. F. & Morris, A., 2011. Timing of uplift of the Troodos Massif (Cyprus) constrained by sedimentary and magnetic polarity evidence. *Journal of the Geological Society*, **168,** 457-470.

Kinnaird, T. *c.* & Robertson, A. H. F., 2013. Tectonic and sedimentary response to incipient diachronous collision of the African and Eurasian plates in southern Cyprus, easternmost Mediterranean region. *In:* Robertson, A. H. F. Parlak, O. Ünlügenç, U. *c.* (eds) Geological Development of Anatolia and the Easternmost Mediterranean Region. *Geological Society, London, Special Publications*, **372,** 585-614.

Kleypas, J. A. Buddemeier, R. W. & Gattuso, J. P., 2001. The future of coral reefs in an age of global change. *International Journal of Earth Sciences*, **90,** 426-437.

Kouwenhoven, T.J., Morigi, C., Negri, A., Giunta, S., Krijgsman, W. & Rouchy, J.M., 2006. Paleoenvironmental evolution of the eastern Mediterranean during the Messinian: Constraints from integrated microfossil data of the Pissouri Basin (Cyprus). *Marine Micropaleontology*, **60**, 17–44.

Krijgsman W., Blanc-Valleron M. M., Flecker R., Hilgen F. J., Kouwenhoven T. J., Orszag-Sperber F., Rouchy J. M., 2002. The onset of the Messinian salinity crisis in the Eastern Mediterranean (Pissouri Basin, Cyprus). *Earth and Planetary Science Letters*, **194**, 299–310.

Lirer, F., Foresi, L. M., Iaccarino, S. M., Salvatorini, G., Turco, E., Cosentino, C., Sierro, F. J. & Caruso, A., 2019. Mediterranean Neogene planktonic foraminifer biozonation and biochronology. Earth-Science Reviews, **196,** 102869.

Lokier, S. W., Wilson, M. E., & Burton, L. M. (2009). Marine biota response to clastic sediment influx: a quantitative approach. Palaeogeography, Palaeoclimatology, Palaeoecology, **281,** 25-42.

Lord, A.R., Panayides, I., Urquhart, E., Xenophontos, *c.* & Malpas, J., 2000. A biochronostratigraphical framework for the Late Cretaceous–Recent circum-Troodos sedimentary sequence, Cyprus. *In: Proceedings of the Third International Conference on the Geology of the Eastern Mediterranean.* Geological Survey Department, Nicosia. **297,** 289-297.

Mankiewicz, C., 1996. The Middle to Upper Miocene carbonate complex of Nijar, Almeria Province. *In:* Franseen, E. K. Esteban, M. Ward, W. *c.* & Rouchy, J. (eds) *Models for Carbonate Stratigraphy from Miocene Reef Complexes of Mediterranean Regions*, Society of Economic Paleontologists and Mineralogists, Tulsa, Oklahoma, 141-157.

Manzi, V., Lugli, S., Roveri, M., Dela Pierre, F., Gennari, R., Lozar, F., Natalicchio, M., Schreiber, B.C., Taviani, M., and Turco, E., 2016. The Messinian salinity crisis in Cyprus: a further step towards a new stratigraphic framework for Eastern Mediterranean. *Basin Research*, **28**, 207–236.

Matteucci R. & Schiavinotto F., 1977. Studio biometrico di *Nephrolepidina*, *Eulepidina* e *Cycloclypeus* in due campioni dell'Oligocene di Monte la Rocca, L'Aquila (Italia Centrale). Geologica Romana, **16**, 141-171.

McArthur, J. M. Howarth, R. J. & Bailey, T. R., 2001. Strontium isotope stratigraphy: LOWESS version 3: best fit to the marine Sr-isotope curve for 0–509 Ma and accompanying look-up table for deriving numerical age. *Journal of Geology*, **109,** 155-170.

McArthur, J. M. & Howarth, R. J., 2004. Sr-isotope stratigraphy. *In:* Gradstein, F.M. Ogg, J.G. and Smith, A.G. (eds) A Geological Timescale, 2004, *Cambridge University Press, Cambridge* 589

McCay, G.A., Robertson, A.H.F., Kroon, D., Raffi, I., Ellam, R.M. & Necdet, M. 2013. Stratigraphy of Cretaceous to Lower Pliocene sediments in the northern part of Cyprus based on comparative 87Sr/86Sr isotopic, nannofossil and planktonic foraminiferal dating. *Geological Magazine*, **150**, 333–359, https://doi.org/10.1017/S0016756812000465.

Meilijson, A., Hilgen, F., Sepúlveda, J., Steinberg, J., Fairbank, V., Flecker, R., Waldmann, N.D., Spaulding, S.A., Bialik, O.M. & Boudinot , F.G., 2019. Chronology with a pinch of salt: Integrated stratigraphy of Messinian evaporites in the deep Eastern Mediterranean reveals long-lasting halite deposition during Atlantic connectivity. *Earth-Science Reviews*, **194**, 374–398.

Miller, K. G., Kominz, M. A., Browning, J. V., Wright, J. D., Mountain, G. S., Katz, M. E. & Pekar, S. F., 2005. The Phanerozoic record of global sea-level change. *Science***, 310**(5752), 1293-1298.

Miller, K.G., Browning, J. V., John Schmelz, W., Kopp, R.E., Mountain, G.S. & Wright, J.D., 2020. Cenozoic sea-level and cryospheric evolution from deep-sea geochemical and continental margin records. *Science Advances*, **6**, https://doi.org/10.1126/sciadv.aaz1346.

Morel, S. W., 1960. The Geology and Mineral Resources of the Apsiou-Akrotiri area, Cyprus Geological Survey Department Memoir, **7**, 51-88.

Mutti, M., Bernoulli, D. & Stille, P., 1997 Temperate carbonate platform drowning linked to Miocene oceanographic events: Maiella platform margin, Italy. *Terra Nova*, **9**, 199-125.

NASA/METI/AIST/Japan Spacesystems, and U.S./Japan ASTER Science Team., 2019. ASTER Global Digital Elevation Model V003 Data set]. NASA EOSDIS Land Processes DAAC. https://doi.org/10.5067/ASTER/ASTGTM.003

Ohneiser, C., Florindo, F., Stocchi, P., Roberts, A.P., DeConto, R.M. & Pollard, D., 2015. Antarctic glacio-eustatic contributions to late Miocene Mediterranean desiccation and reflooding. *Nature Communications*, **6**, 8765, https://doi.org/10.1038/ncomms9765.

Oosterbaan, A.F.F., 1988. Early Miocene corals from the Aquitaine Basin (SW France). *Mededelingen van de Werkgroep voor Tertiaire en Kwartaire Geologie*, **25**, 247-284.

Oosterbaan, A.F.F., 1990. Notes on a collection of Badenian (Middle Miocene) corals from Hungary in the National Museum of Natural History at Leiden (the Netherlands). *Mededelingen van de Werkgroep voor Tertiaire en Kwartaire Geologie*, **27**, 3–15.

Orszag-Sperber, F., Rouchy, J.M. & Elion, P., 1989. The sedimentary expression of regional tectonic events during the Miocene-Pliocene transition in the southern Cyprus basins. *Geological Magazine*, 126, 291–299.

Orszag-Sperber, F., Caruso, A., Blanc-Valleron, M.M., Merle, D. & Rouchy, J.M., 2009. The onset of the Messinian salinity crisis: Insights from Cyprus sections. *Sedimentary Geology*, **217**, 52–64.

Özcan, E. & Less, G., 2009. First record of the co-occurrence of western Tethyan and Indo-Pacific larger foraminifera in the Burdigalian of the Mediterranean province. *The Journal of Foraminiferal Research*, **39**, 23-39.

Özcan, E., Less, G., Báldi-Beke, M., Kollányi, K. & Acar, F., 2009. Oligo-Miocene foraminiferal record (Miogypsinidae, Lepidocyclinidae and Nummulitidae) from the Western Taurides (SW Turkey): biometry and implications for the regional geology. Journal of Asian Earth Sciences, **34,** 740-760.

Özcan, E., Less, G., Okay, A. I., Baldi-Beke, M., Kollányi, K., & Yilmaz, İ. Ö., 2010. Stratigraphy and larger foraminifera of the Eocene shallow-marine and olistostromal units of the southern part of the Thrace Basin, NW Turkey. *Turkish Journal of Earth Sciences*, **19,** 27-77.

Palamakumbura, R.N., Robertson, A.H.F., Kinnaird, T.C., van Calsteren, P., Kroon, D. & Tait, J.A., 2016. Quantitative dating of Pleistocene deposits of the Kyrenia range, Northern Cyprus: Implications for timing, rates of uplift and driving mechanisms. *Journal of the Geological Society*, **173**, 933–948.

Papadimitriou, N., Deschamps, R., Symeou, V., Souque, C., Gorini, C., Nader, F.H. & Blanpied, C., 2018. The tectonostratigraphic evolution of Cenozoic basins of the Northern Tethys: The Northern margin of the Levant Basin. *Oil and Gas Science and Technology*, **73**, (77), https://doi.org/10.2516/ogst/2018085.

Payne, A. S. & Robertson, A. H. F., 1995. Neogene supra-subduction zone extension in the Polis graben system, west Cyprus. *Journal of the Geological Society*, **152,** 613-628.

Payne, A. S. & Robertson, A. H. F., 2000. Structural evolution and regional significance of the Polis graben system, western Cyprus. *In:* Panayiotou A. (ed) *Proceedings of the Third International Conference on the Geology of the Eastern Mediterranean*, Geological Survey Department, Nicosia, Cyprus, 45-59.

Pearce, J.A. & Robinson, P.T., 2010. The Troodos ophiolitic complex probably formed in a subduction initiation, slab edge setting. *Gondwana Research*, **18**, 60–81.

Pedley, H. M., 1979. Miocene bioherms and associated structures in the Upper Coralline limestone of the Maltese Islands: their lithification and palaeoenvironment. Sedimentology, **26,** 577-591.

Pedley, H. & Grasso, M. 1994. A model for the late Miocene reef-Tripolaceous associations of Sicily and its relevance to aberrant coral growth-forms and reduced biological diversity within the Palaeomediterranean. *Geologie Mediterraneenne*, **21**, 109–121, https://doi.org/10.3406/geolm.1994.1501.

Perrin *c.* & Bosellini F., 2012. Paleobiogeography of scleractinian reef corals: Changing patterns during the Oligocene–Miocene climatic transition in the Mediterranean. Earth-Science Reviews, **111,** 1-24.

Riegel, B. & Piller, W.E., 2000. Biostromal Coral Facies—A Miocene Example from the Leitha Limestone (Austria) and its Actualistic Interpretation. *PALAIOS*, **15**, 399–413.

Polissar, P.J., Rose, C., Uno, K.T., Phelps, S.R. & deMenocal, P. 2019. Synchronous rise of African C4 ecosystems 10 million years ago in the absence of aridification. Nature Geoscience, 12, 657–660, https://doi.org/10.1038/s41561-019-0399-2.

Pomar, L. Ward, W. *c.* & Green, D. G., 1996. Upper Miocene reef complex of the Llucmajor area, Mallorca, Spain. *In:* Franseen, E.K., Esteban M., Ward W.C.& Rouchy J.M. (eds) Models for Carbonate Stratigraphy from Miocene Reef complexes of the Mediterranean area. *Concepts in Sedimentology and Paleontology*, **5**, Society for Sedimentary Geology, Tulsa, Oklaoma, U.S.A, **5, 19**1–225.

Pomar, L., Bassant, P., Brandano, M., Ruchonnet, C., & Janson, X., 2012. Impact of carbonate producing biota on platform architecture: insights from Miocene examples of the Mediterranean region. Earth-Science Reviews, **113**, 186-211.

Pomar, L., Mateu-Vicens, G., Morsilli, M. & Brandano, M., 2014. Carbonate ramp evolution during the late Oligocene (Chattian), Salento Peninsula, southern Italy. Palaeogeography, Palaeoclimatology, Palaeoecology, **404**, 109-132.

Pomar, L., Baceta, J.I., Hallock, P., Mateu-Vicens, G., Basso, D., 2017. Reef building and carbonate production modes in the west-central Tethys during the Cenozoic. *Marine and Petroleum Geology*, **83,** 261-304.

Prista, G. A., Agostinho, R. J. & Cachão, M. A., 2015. Observing the past to better understand the future: a synthesis of the Neogene climate in Europe and its perspectives on present climate change. Open Geosciences, 1 (open-issue). https://doi.org/10.1515/geo-2015-0007

Reinhold, C., 1995. Guild structure and aggradation pattern of Messinian Porites patch reefs: ecological succession and external environmental control (San Miguel de Salinas Basin, SE Spain). *Sedimentary Geology*, **97**, 157–175.

Robertson, A. H. F., 1977a. Tertiary uplift history of the Troodos massif, Cyprus. *Geological Society of America Bulletin*, **88,** 1763-1772.

Robertson, A. H. F., 1977b. The Kannaviou Formation, Cyprus: volcaniclastic sedimentation of a probable late Cretaceous volcanic arc. *Journal of the Geological Society*, **134,** 269-292.

Robertson, A.H.F., 1990. Tectonic evolution of Cyprus. *In:* J. Malpas, E.M. Moores, A. Panayiotou, *c*. Xenophontos (eds.), Ophiolites Oceanic Crustal Analogues, Proc. Symp. 'Troodos 1987', Geological Survey Department, Cyprus. 235-252.

Robertson, A. H., 1998a. Tectonic significance of the Eratosthenes Seamount: a continental fragment in the process of collision with a subduction zone in the eastern Mediterranean (Ocean Drilling Program Leg 160). Tectonophysics**, 298**, 63-82.

Robertson A.H.F., 1998b. Miocene shallow-water carbonates on the Eratosthenes Seamount, easternmost Mediterranean Sea. *In:* Robertson, A.H.F., Emeis, K.C., Richter, C., Camerlenghi, A. (eds) Proceedings of the Ocean Drilling Program, Scientific Results, **160**, 419-436.

Robertson, A. H. F., Boulton, S.J., Taslı, K., Yıldırım, N., İnan, N., Yıldız, A. & Parlak, O., 2016. Late Cretaceous–Miocene sedimentary development of the Arabian continental margin in SE Turkey (Adıyaman region): Implications for regional palaeogeography and the closure history of Southern Neotethys. *Journal of Asian Earth Sciences*, **115**, 571–616.

Robertson, A. H. F., Parlak, O. & Ustaömer, T., 2012. Overview of the Palaeozoic–Neogene evolution of Neotethys in the Eastern Mediterranean region (southern Turkey, Cyprus, Syria). *Petroleum Geoscience*, **18,** 381-404.

Robertson, A. H. F., Eaton, S., Follows, E. J. & McCallum, J. E., 1991. The role of local tectonics versus global sea-level changes in the Neogene evolution of the Cyprus active margin. *In:* Macdonald, D.I.M. (ed) *Sedimentation, Tectonics and Eustasy: Sea-level Changes at Active Margins*, Special Publication of the International Association of Sedimentologists, **12**, 331-369.

Robertson, A.H.F., Eaton, S., Follows, E.J. & Payne, A.S. 1995. Depositional processes and basin analysis of Messinian evaporites in Cyprus. *Terra Nova*, **7**, 233–253.

Robertson, A.H.F & Xenophontos, *c*. 1993. Development of concepts concerning the Troodos ophiolite and adjacent units in Cyprus. *Geological Society, London, Special Publications*, **76**, 85–119.

Rögl F., 1999. Mediterranean and Paratethys facts and hypotheses of an Oligocene to Miocene paleogeography (short overview). *Geologica Carpathica*, **50,** 339-349.

Rouchy, J.-M., Saint Martin, J.-P., Maurin, A. & Bernet-Rollande, M.-C., 1986. Evolution et antagonisme des communautés bioconstructrices animales et végetalés à la fin du Miocène en Mediterranée occidentale: biologie et sédimentologie. *Bulletin du Centre de Recherche Exploration et Production Elf Aquitaine*, **10**, 333–348.

Roveri, M., Flecker, R., Krijgsman, W., Lofi, J., Lugli, S., Manzi, V., Sierro, F. J., Bertini, A., Camerlenghi, A., De Lange, G., Govers, R., Hilgen, J. J., Hübscher, C., Meijer, P. Th., Stoica, M., 2014. The Messinian Salinity Crisis: Past and future of a great challenge for marine sciences. *Marine Geology*, **352**, 25–58.

Saint-Martin, J. P., & Rouchy, J. M., 1990. Les plateformes carbonatées méssiniennes en Mediterranée occidentale; leur importance pour la reconstitution des variations du niveau marin au Miocene terminal. Bulletin de la Société géologique de France, 6(1), 83-94.

Şafak, U., Kelling, G., Gökçen, N.S. & Gürbüz, K., 2005. The mid- Cenozoic succession and evolution of the Mut basin, southern Turkey, and its regional signicance. *Sedimentary Geology*, **173**, 121–150.

Schlager, W., 1994. Highstand shedding of carbonate platforms, *Journal of Sedimentary Research*, **64**, 270-281.

Schlager, W., 1999. Scaling of sedimentation rates and drowning of reefs and carbonate platforms, *Geology*, **27**, 183-186.

Schuster, F. 2002a. Oligocene and Miocene examples of Acropora-dominated palaeoenvironments: Mesohellenic Basin (NW Greece) and northern Gulf of Suez (Egypt). *Proceedings of the 9th International Coral Reefs Symposium*, Bali, Indonesia, **1**, 199–204.

Schuster, F. 2002b. Early Miocene corals and associated sediments of the northwestern Gulf of Suez, Egypt. *Courier Forschungsinst. Senckenberg*, **239**, 57–81.

Spezzaferri, S., Cita, M. B. & McKenzie, J. A., 1998. The Miocene/Pliocene boundary in the Eastern Mediterranean: results from Sites 967 and 969. *In*: Robertson, A. H. F. Emeis, K. *c.* Richter, *c.* Camerlenghi, A. (eds) Proceedings, Ocean Drilling Program Scientific Results, **160,** 9-28, National Science Foundation.

Spezzaferri S. & Tamburini F., 2007. Paleodepth variations on the Eratosthenes Seamount (Eastern Mediterranean): sea level changes or subsidence? *Earth Discussions*, **2**, 115-132.

Swarbrick, R. E. & Naylor, M. A., 1980. The Kathikas Melange, SW Cyprus: late Cretaceous submarine debris flows. *Sedimentology*, **27,** 63-78.

Taylforth J.E., McCay G.A., Ellam R., Raffi I., Kroon D., Robertson A.H.F., 2014. Middle Miocene (Langhian) sapropel formation in the easternmost Mediterranean deep-water basin: Evidence from northern Cyprus. *Marine and Petroleum Geology***, 57,** 521-536.

Tomassetti, L., Bosellini, F.R., Brandano, M., 2013. Growth and demise of a Burdigalian coral bioconstruction on a granite rocky substrate (Bonifacio Basin, south-eastern Corsica). *Facies*, **59,** 703-716.

Toomey, M., Ashton, A.D. & Perron, J.T., 2013. Profiles of ocean island coral reefs controlled by sea-level history and carbonate accumulation rates. *Geology*, **41**, 731–734.

Toscano, M.A. & Macintyre, I.G., 2003. Corrected western Atlantic sea-level curve for the last 11,000 years based on calibrated 14C dates from Acropora palmata framework and intertidal mangrove peat. *Coral Reefs*, **22**, 257–270.

Tzanova, A., Herbert, T. D., & Peterson, L. (2015). Cooling Mediterranean Sea surface temperatures during the Late Miocene provide a climate context for evolutionary transitions in Africa and Eurasia. *Earth and Planetary Science Letters*, **419**, 71–80. https://doi.org/https://doi.org/10.1016/j.epsl.2015.03.016

Vertino, A., Stolarski, J., Bosellini, F.R. & Taviani, M., 2014. Mediterranean Corals Through Time: From Miocene to Present. *In*: Goffredo, S. & Dubinsky, Z. (eds) *The Mediterranean Sea: Its History and Present Challenges*. Dordrecht, Springer Netherlands, 257–274.

Vescogni, A., Bosellini, F. R., Reuter, M. & Brachert, T. C., 2008. Vermetid reefs and their use as palaeobathymetric markers: New insights from the Late Miocene of the Mediterranean (Southern Italy, Crete). *Palaeogeography, Palaeoclimatology, Palaeoecology*, **267**, 89-101.

Vescogni, A., Bosellini, F. R., Cipriani, A., Gürler, G., Ilgar, A. & Paganelli, E., 2014. The Dağpazarı carbonate platform (Mut Basin, Southern Turkey): Facies and environmental reconstruction of a coral reef system during the Middle Miocene Climatic Optimum. *Palaeogeography, Palaeoclimatology, Palaeoecology*, **410**, 213-232.

Wade, B. S. Pearson, P. N. Berggren, W. A. & Pälike, H., 2011. Review and revision of Cenozoic tropical planktonic foraminiferal biostratigraphy and calibration to the geomagnetic polarity and astronomical time scale. *Earth-Science Reviews,* **104,** 111-142.

Westerhold, T., Bickert, T. & Röhl, U., 2005. Middle to late Miocene oxygen isotope stratigraphy of ODP site 1085 (SE Atlantic): New constrains on Miocene climate variability and sea-level fluctuations. *Palaeogeography, Palaeoclimatology, Palaeoecology*, **217**, 205–222.

Wilson, M. E., & Lokier, S. W., 2002. Siliciclastic and volcaniclastic influences on equatorial carbonates: insights from the Neogene of Indonesia. Sedimentology, **49,** 583-601.

Ylmaz Y., 1993. New evidence and model on the evolution of the southeast Anatolian orogen. *Geological Society of America Bulletin*, **105,** 251-271.

Zachos, J., Pagani, M., Sloan, L., Thomas, E. & Billups, K., 2001. Trends, rhythms, and aberrations in global climate 65 Ma to present. Science, **292**(5517), 686-693.

Zachos, J. *C.*, Dickens, G. R. & Zeebe, R. E., 2008. An early Cenozoic perspective on greenhouse warming and carbon-cycle dynamics. Nature, **451**(7176), 279-283.

Figure Captions

Fig. 1. Sketch map of the Mediterranean region showing key occurrences of Early, Middle and Late Miocene reef and related facies referred to in this study, including NW Cyprus. 1. Terra Member, Cyprus (this study and literature cited in text); 2. Zincir Kaja Platform, Mut Basin, S Turkey (Bassant *et al*., 2005; Janson *et al*., 2010; Pomar *et al*., 2012); 3. NW Gulf of Suez (Egypt) (Schuster, 2002a, Schuster, 2002b); 4. Paros Island, Greece (Bosellini & Perrin, 2008); 5. Sirt Basin, Libya (Hladil *et al*, 1991); 6. Dolianova, Sardinia, Italy (Cherchi *et al*., 2000; Galloni *et al*., 2001); 7. N Sardinia, Italy (Benisek *et al*., 2009); 8. Bonifacio Basin, Corsica, France (Galloni *et al*., 2001; Tomassetti *et al*., 2013; Brandano *et al*., 2016); 9. Torino Hills, Piedmont, N Italy (Chevalier, 1962); 10. Aquitaine region, S France (Chevalier,

1962; Cahauzac & Chais, 1996); 11. Dağpazarı Platform, Mut Basin, S Turkey (Bassant *et al*., 2005; Janson *et al*., 2010; Pomar *et al*., 2012; Vescogni *et al*., 2014); 12. Ziqlag Formation, Israel (Buchbinder *et al*., 1993); 13. N Hungary (Oosterbaan, 1990); 14. Vienna Basin, Austria (Riegel & Piller, 2000); 15. Torino Hills, Piedmont, N Italy (Chevalier, 1962); 16. Djebel Chott platform, N Algeria (Belkebir *et al*., 1994); 17. Aquitaine region, S France (Chevalier, 1962; Cahauzac & Che, 1996); 18. Valencia Region, E Spain (Calvet *et al*., 1994); 19. Almeria, S Spain (Mankiewicz, 1996); 20. Murchas, Granada Basin, S Spain (Braga *et al*., 1996); 21. Koronia Member, Cyprus (this study and literature cited in text); 22. Pattish Formation, Israel (Buchbinder *et al*., 1993; Buchbinder & Zilberman, 1997); 23. Kasaba Formation, SW Turkey (Hayward *et al*., 1996); 24. Crete, Greece (Brachert *et al*., 2006); 25. Sirt Basin, Libya (Hladil *et al*, 1991); 26. Salento Peninsula, Apulia, S Italy (Bosellini *et al*., 2001; Bosellini *et al*., 2002; Bosellini, 2006; Vescogni *et al*., 2008)); 27. Calabria, S Italy (Chavalier, 1962; Pedley & Grasso, 1994); 28. Malta (Pedley, 1979); 29. Maiella Mountain, Abruzzo, Italy (Danese, 1999; Civitelli & Brandano); 30. Lampedusa, Pelagian Islands, S Italy (Grasso & Pedley,1985); 31. Livorno Hills, Tuscany, Italy (Bossio *et al*., 1996); 32. Llucmajor Platform, Mallorca, Spain (Pomar *et al*., 1996); 33. San Miguel de Salinas Basin, SE Spain (Reinhold, 1995); 34. Almeria, S Spain (Brachert *et al*.,1996; Mankiewicz, 1996); 35. Melilla, N Morocco (Rouchy *et al*., 1986); 36. Granada Basin, S Spain (Braga & Aguirre, 2001). For a more complete catalogue of Mediterranean reef occurrences see Bosellini & Perrin, 2008.

Fig. 2. Outline geological map of Cyprus showing the location of the Polis graben and related reef units in NW Cyprus and other Miocene reef-related units in Cyprus (Modified from Kinnaird *et al.*, 2011). Note that many of the outcrops are dominated by reef-related talus. Inset: tectonic setting of Cyprus in the eastern Mediterranean shown (modified from Follows & Robertson, 1990; Robertson *et al.*, 1991 and Payne, 1995).

Fig. 3. Revised geological map of NW Cyprus, focussing on the Miocene facies (modified from Constantinou, 1995; Follows *et al.*, 1996 and Balmer *et al.,* 2019). Major faults of the Polis Graben are Payne & Robertson (1995).

Fig. 4. Sedimentary logs for key sections on the east and west flanks of the Polis graben, selected for age dating. See Fig. 5 for locations and the text for explanation.

Fig. 5. Topographic map of NW Cyprus (produced using ASTER Global Digital Elevation Model V003) showing the locations of the samples used for dating by different methods. Planktic foraminifera were sampled more generally (see supplementary material table S3).

Fig. 6. Stratigraphic interpretation focussing on the Miocene of NW Cyprus, as exposed on the east and west flanks of the Polis graben and in the intervening depocentre (modified after Follows *et al.* (1996), Payne & Robertson (1995), Balmer *et al.* (2019) and this study).

Fig. 7. Schematic cross-section of the northern Polis graben showing the distribution of units in relation to the present-day topography (based on Payne & Robertson, 1995, 2000). Note the Koronia Member, the Terra Member and the Pakhna Formation (undifferentiated). Key sample locations during this study are projected onto the section. See Fig. 3 for the approximate line of section.

Fig. 8. Field photographs of key Miocene facies from the west flank of the Polis graben. a, Rhythmical alternations of hemipelagic marl and chalk (above debris flow-deposit shown in b, c); correlated with the Mid-Miocene redeposited facies (see Fig. 3); Kouroulla Gorge, NW Akamas Peninsula; b, Debris-flow interbedded with hemipelagic marl and chalk (beneath a); c, Detail of the debris-flow unit in b. Based on dating, some of the intraclasts of marl and chalk (and smaller extraclasts) are likely to have been eroded from beneath the Miocene succession; d, Faviid coral fragment from the debris-flow deposit shown in b, c; e, Faviid corals in reworked Terra Member talus; Androlikou Quarry; f, Poritid coral, typical of the Koronia Member; near Akamas Village; Akamas Peninsula; g, Neptunian dykes cutting the karstified, uppermost surface of the Koronia Member, infilled with pink Pliocene marl; near Pelathousa; NE Polis graben.

Fig. 9. Detailed log of part of the interval of hemipelagic sediments and debris-flow deposits exposed in Kouroulla Gorge (see Fig. 4, log. 1). Samples were dated from below and above the discrete debris flow-deposit.

Fig. 10. Photomicrographs of two coralline algae-rich packstones with benthic foraminifera; from the west flank of the Polis graben (see Fig. 9): A. Sample TC1749, Early Miocene Terra Member; white arrowhead indicates *Eulepidina* sp.; B. Sample TC1746, Late Oligocene

neritic facies, White arrowhead indicates *Borelis melo melo*; black arrow indicates *Dendritina* sp..

Fig. 11. Sr age data for, 19 samples (in order of collection location East to West) of marl and chalk; collected from selected intervals of the Polis graben (see Fig. 5), plotted against absolute age. The determined age and the total combined error are shown for each sample. The time scale used is that of Cohen *et al.,* 2020.

Fig 12. Summary of the inferred age versus sedimentation based on this study. A. Upper Lefkara Formation (pelagic carbonates) (Lord *et al.,* 2000); B. Neritic carbonates (un-named formation) (NW Akamas Peninsula) (this study); *c.* Undifferentiated Pakhna Formation. (mainly marl and chalk) (this study); D. Terra Member. Reef and related neritic sediments (Follows *et al.,* 1996; this study); E. Middle Miocene redeposited and hemipelagic carbonates (this study); F. Koronia Member (Follows *et al.,* 1996; this study).

Fig. 13. Reconstruction of basin development including the coral reefs and related facies. (A) Early Miocene. The Terra Member reefs develop on a local topographic high in NW Cyprus (Akamas Peninsula), prior to formation of a well-defined graben; virtually no *in situ* reef is now preserved; (B) Late Miocene. The Koronia Member reefs develop on the upfaulted flanks of the Polis graben; *in situ* reef material is mainly restricted to the Akamas Peninsula. A is *c.* 10km N of section B.

Fig. 14. Benthic $\delta^{18}O$ data for the interval of the Middle Miocene Climate Transition (from the South China Sea), with the range of debris flow deposition in Kouroulla Gorge shown (after Holburn *et al.*, 2018).

Figure 1 Click here to access/download;figure;Fig 1 - Miocene Med reef map.pdf

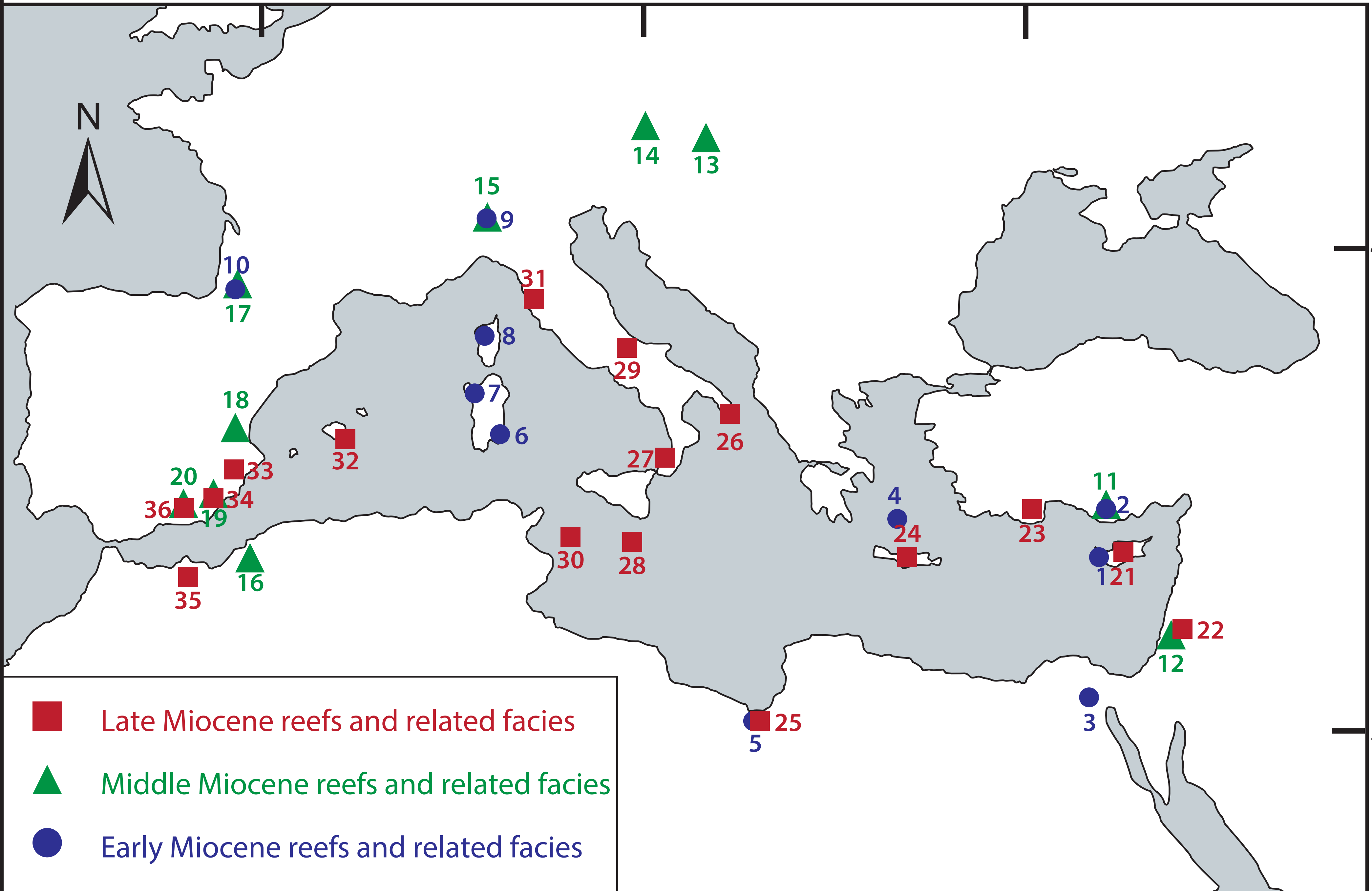

Figure 2

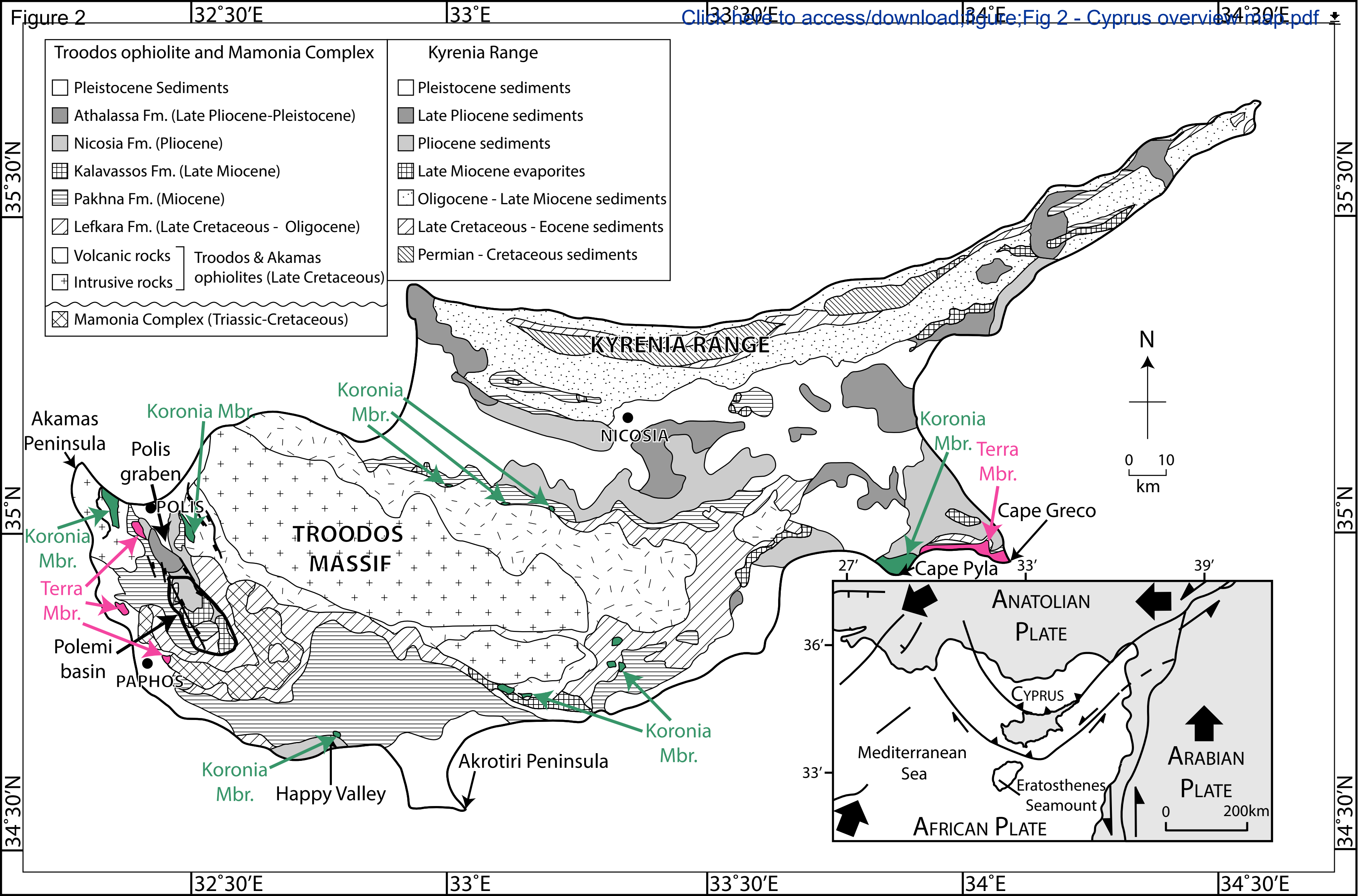
Troodos ophiolite and Mamonia Complex
Pleistocene Sediments
Athalassa Fm. (Late Pliocene-Pleistocene)
Nicosia Fm. (Pliocene)
Kalavassos Fm. (Late Miocene)
Pakhna Fm. (Miocene)
Lefkara Fm. (Late Cretaceous - Oligocene)
Volcanic rocks
Intrusive rocks
Troodos & Akamas ophiolites (Late Cretaceous)
Mamonia Complex (Triassic-Cretaceous)
Kyrenia Range
Pleistocene sediments
Late Pliocene sediments
Pliocene sediments
Late Miocene evaporites
Oligocene - Late Miocene sediments
Late Cretaceous - Eocene sediments
Permian - Cretaceous sediments
32°30′E
33°E
33°30′E
34°E
34°30′E
35°30′N
35°N
34°30′N
KYRENIA RANGE
NICOSIA
TROODOS MASSIF
Akamas Peninsula
Polis graben
POLIS
Polemi basin
PAPHOS
Koronia Mbr.
Terra Mbr.
Cape Greco
Cape Pyla
Happy Valley
Akrotiri Peninsula
N
0 10
km
27′
33′
39′
36′
33′
ANATOLIAN PLATE
CYPRUS
Mediterranean Sea
Eratosthenes Seamount
AFRICAN PLATE
ARABIAN PLATE
0 200km

Figure 3

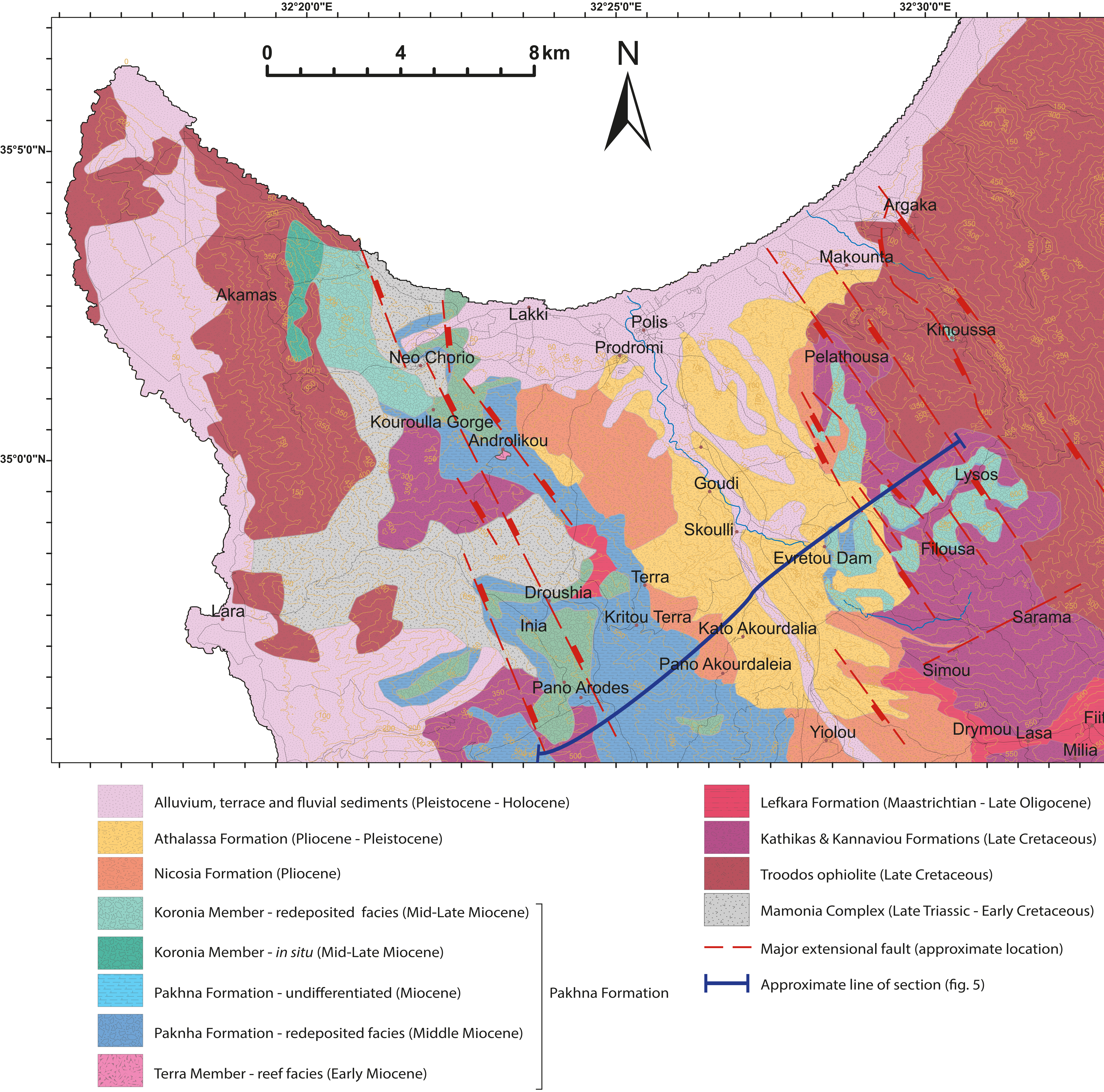

32°20'0"E
32°25'0"E
32°30'0"E
35°5'0"N
35°0'0"N
0
4
8 km
N
Akamas
Lakki
Polis
Prodromi
Neo Chorio
Kouroulla Gorge
Androlikou
Argaka
Makounta
Kinoussa
Pelathousa
Goudi
Skoulli
Lysos
Evretou Dam
Filousa
Terra
Droushia
Lara
Inia
Kritou Terra
Kato Akourdalia
Sarama
Pano Akourdaleia
Simou
Pano Arodes
Yiolou
Drymou
Lasa
Fiiti
Milia
Alluvium, terrace and fluvial sediments (Pleistocene - Holocene)
Athalassa Formation (Pliocene - Pleistocene)
Nicosia Formation (Pliocene)
Koronia Member - redeposited facies (Mid-Late Miocene)
Koronia Member - in situ (Mid-Late Miocene)
Pakhna Formation - undifferentiated (Miocene)
Paknha Formation - redeposited facies (Middle Miocene)
Terra Member - reef facies (Early Miocene)
Pakhna Formation
Lefkara Formation (Maastrichtian - Late Oligocene)
Kathikas & Kannaviou Formations (Late Cretaceous)
Troodos ophiolite (Late Cretaceous)
Mamonia Complex (Late Triassic - Early Cretaceous)
Major extensional fault (approximate location)
Approximate line of section (fig. 5)

Figure 4

Click here to access/download;figure;Fig 4 - Facies logs.pdf

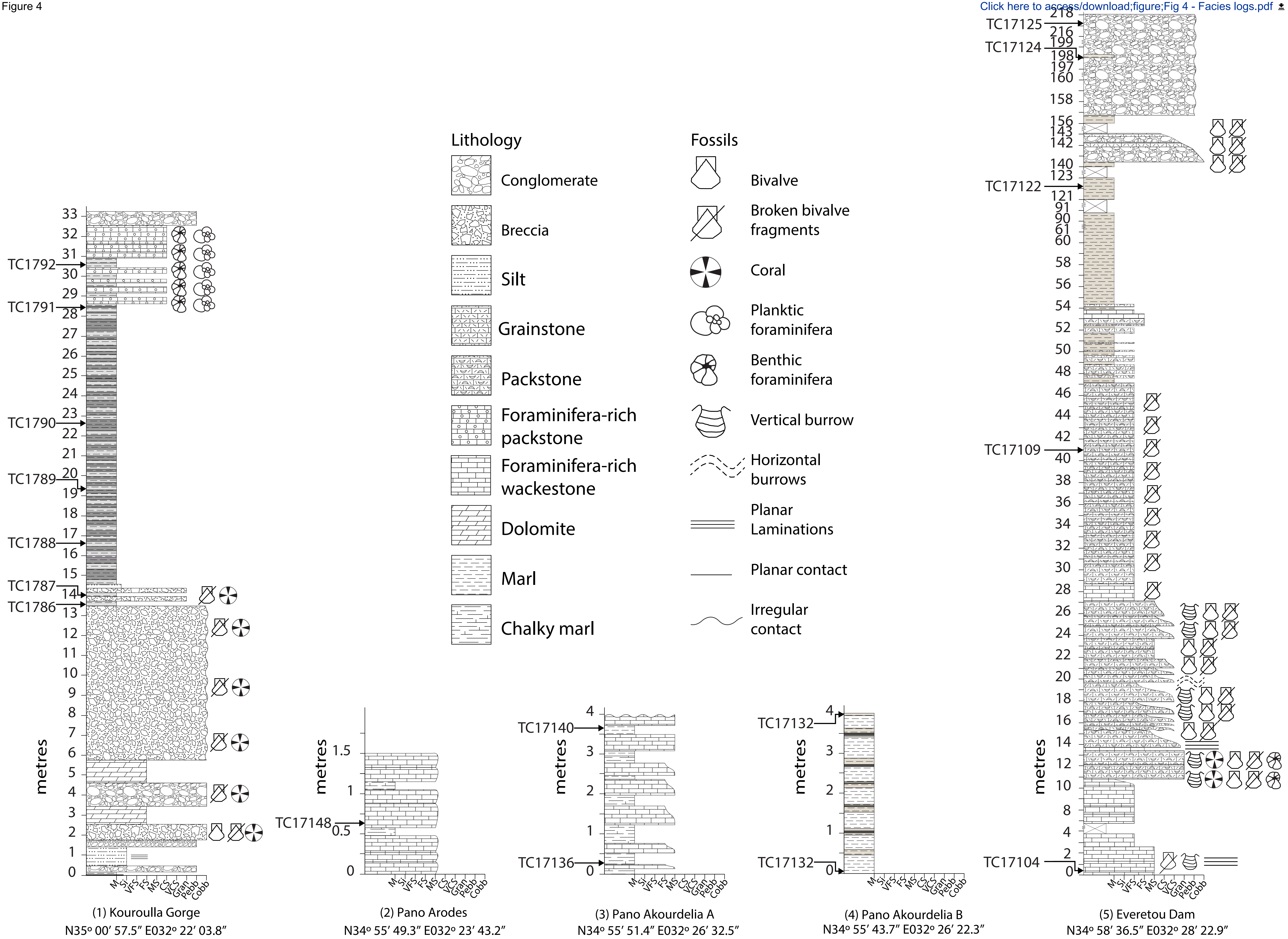

Figure 5

Click here to access/download;figure;Fig 5 - Locality Map.pdf

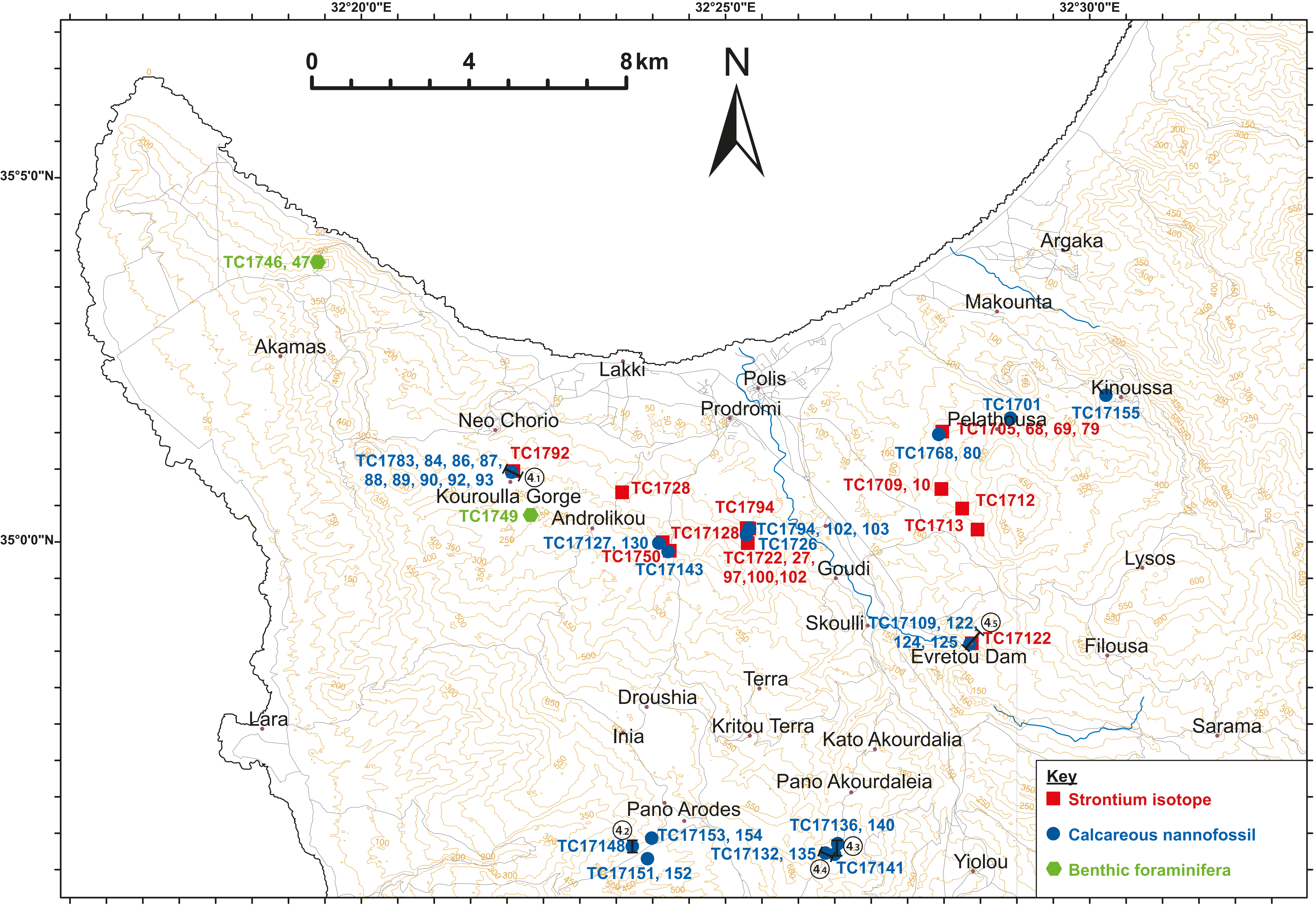

Figure 6

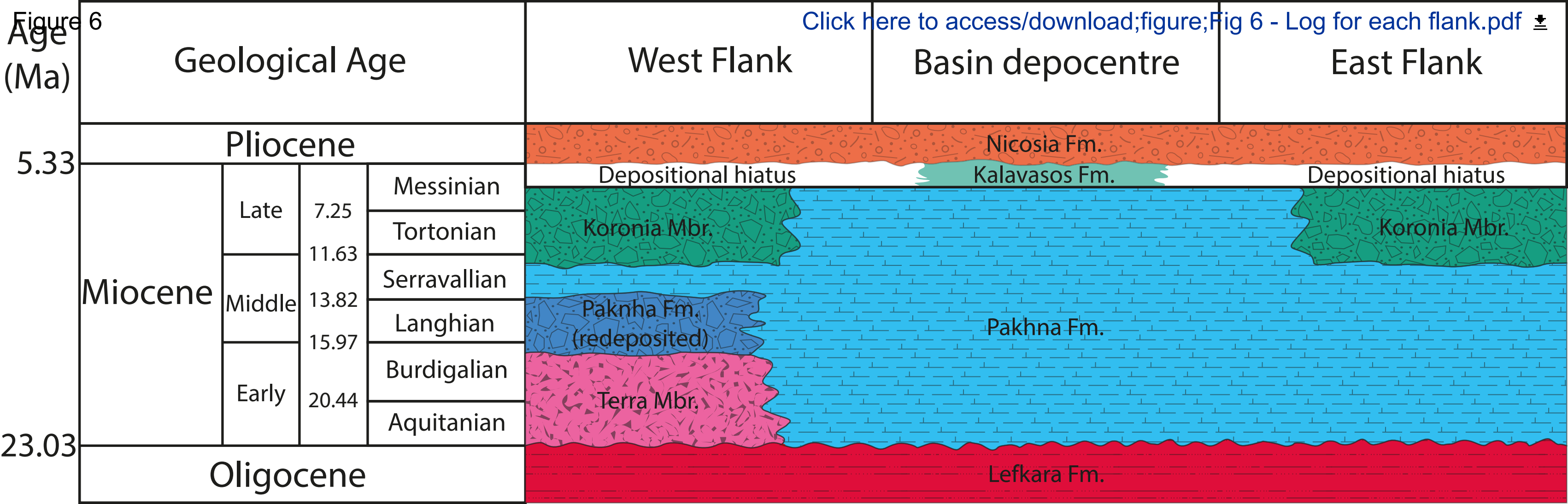

Age (Ma)
Geological Age
West Flank
Basin depocentre
East Flank
Pliocene
5.33
Nicosia Fm.
Depositional hiatus
Kalavasos Fm.
Depositional hiatus
Miocene
Late
7.25
Messinian
Tortonian
11.63
Koronia Mbr.
Koronia Mbr.
Middle
Serravallian
13.82
Paknha Fm. (redeposited)
Langhian
Pakhna Fm.
15.97
Burdigalian
Early
20.44
Terra Mbr.
Aquitanian
23.03
Oligocene
Lefkara Fm.

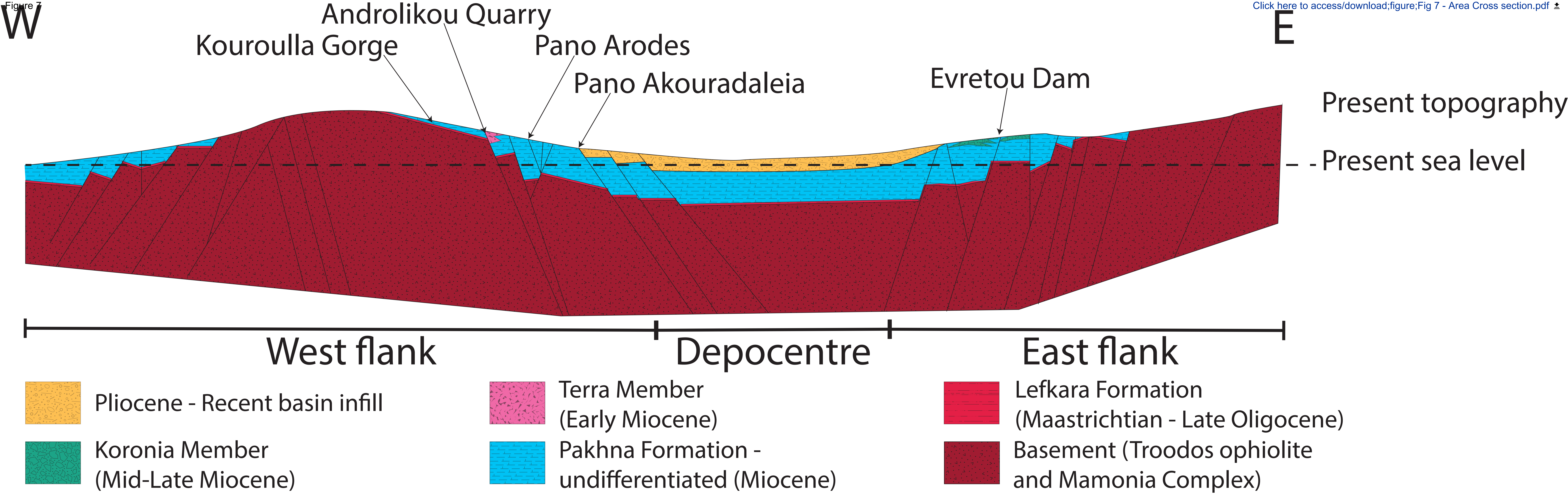
W
E
Androlikou Quarry
Kouroulla Gorge
Pano Arodes
Pano Akouradaleia
Evretou Dam
Present topography
Present sea level
West flank
Depocentre
East flank
Pliocene - Recent basin infill
Koronia Member
(Mid-Late Miocene)
Terra Member
(Early Miocene)
Pakhna Formation -
undifferentiated (Miocene)
Lefkara Formation
(Maastrichtian - Late Oligocene)
Basement (Troodos ophiolite
and Mamonia Complex)

Figure 8

Figure 9

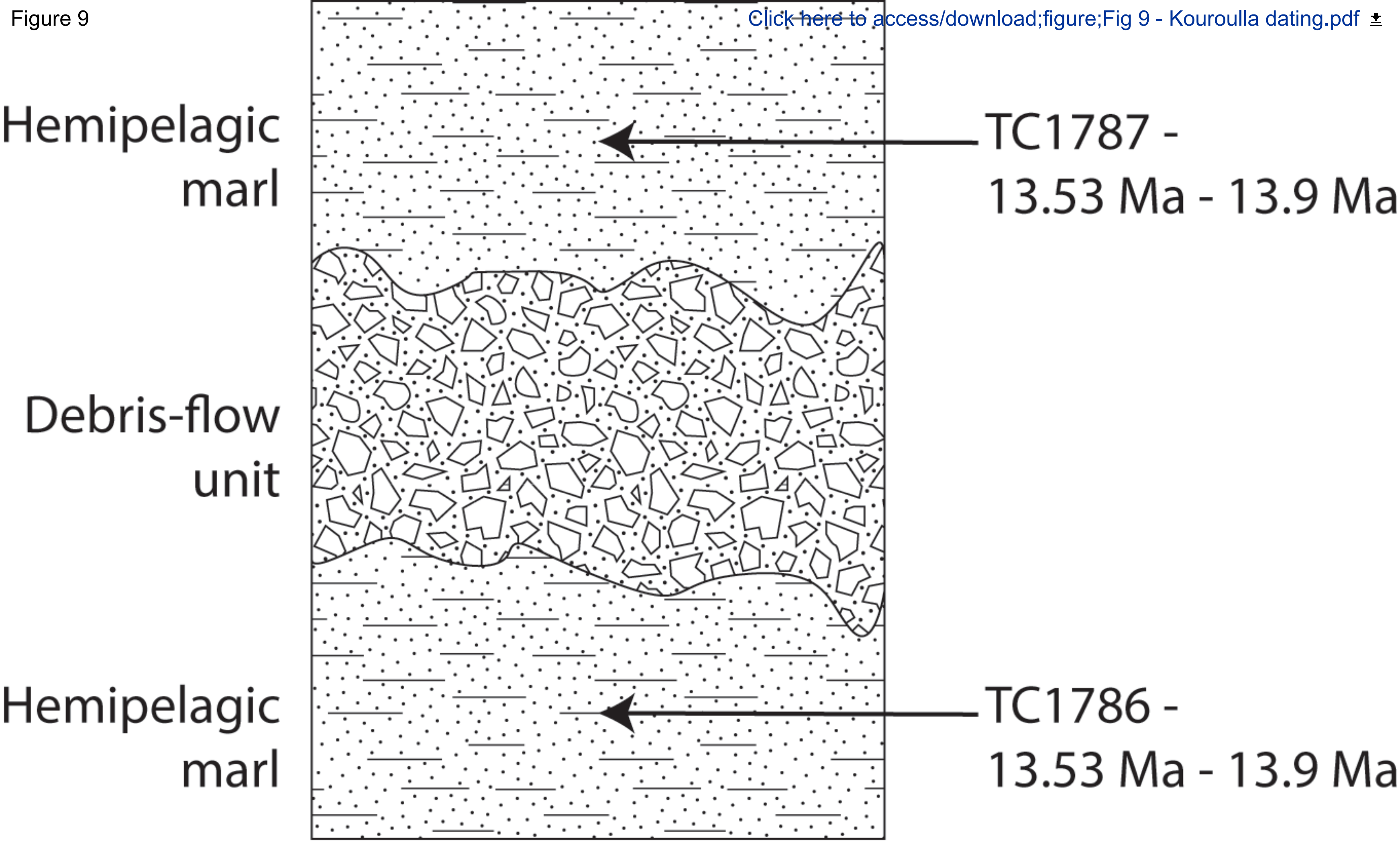
Hemipelagic marl
TC1787 -
13.53 Ma - 13.9 Ma
Debris-flow unit
Hemipelagic marl
TC1786 -
13.53 Ma - 13.9 Ma

Figure 10

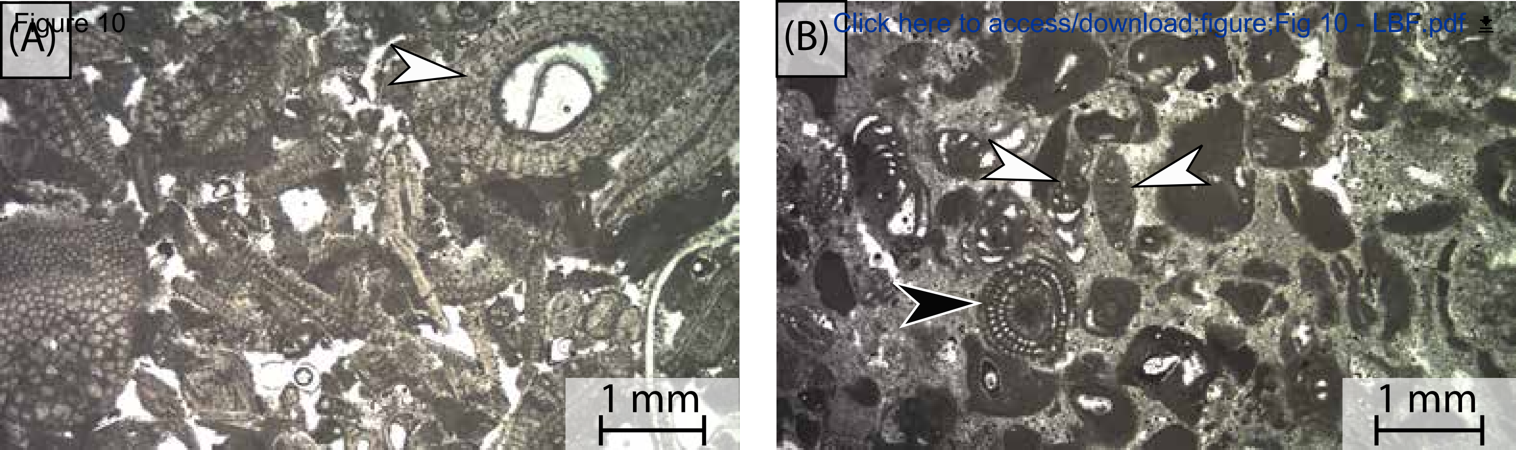

Figure 11

Click here to access/download;figure;Fig 11 - Sr Graph.pdf

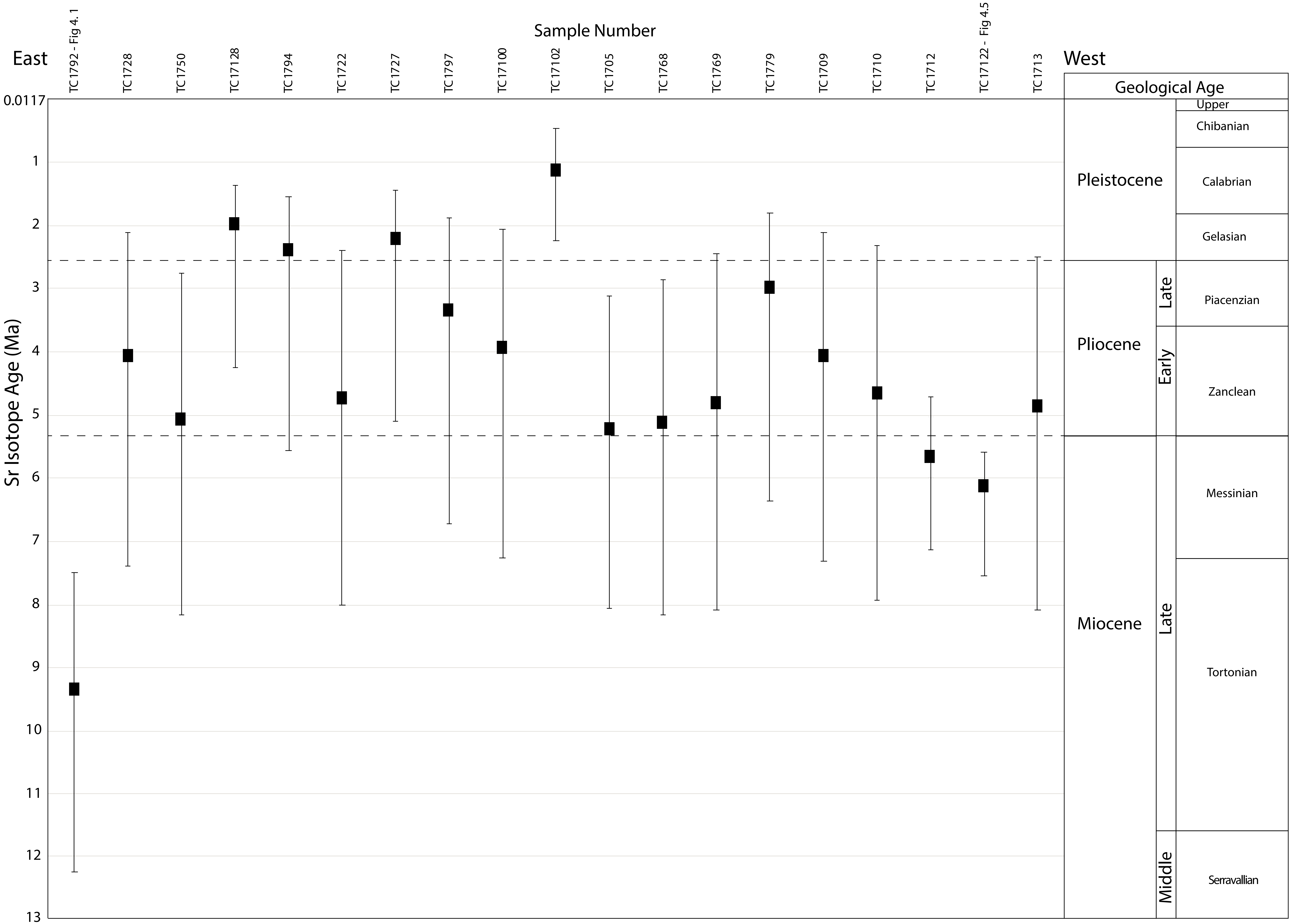

Figure 12

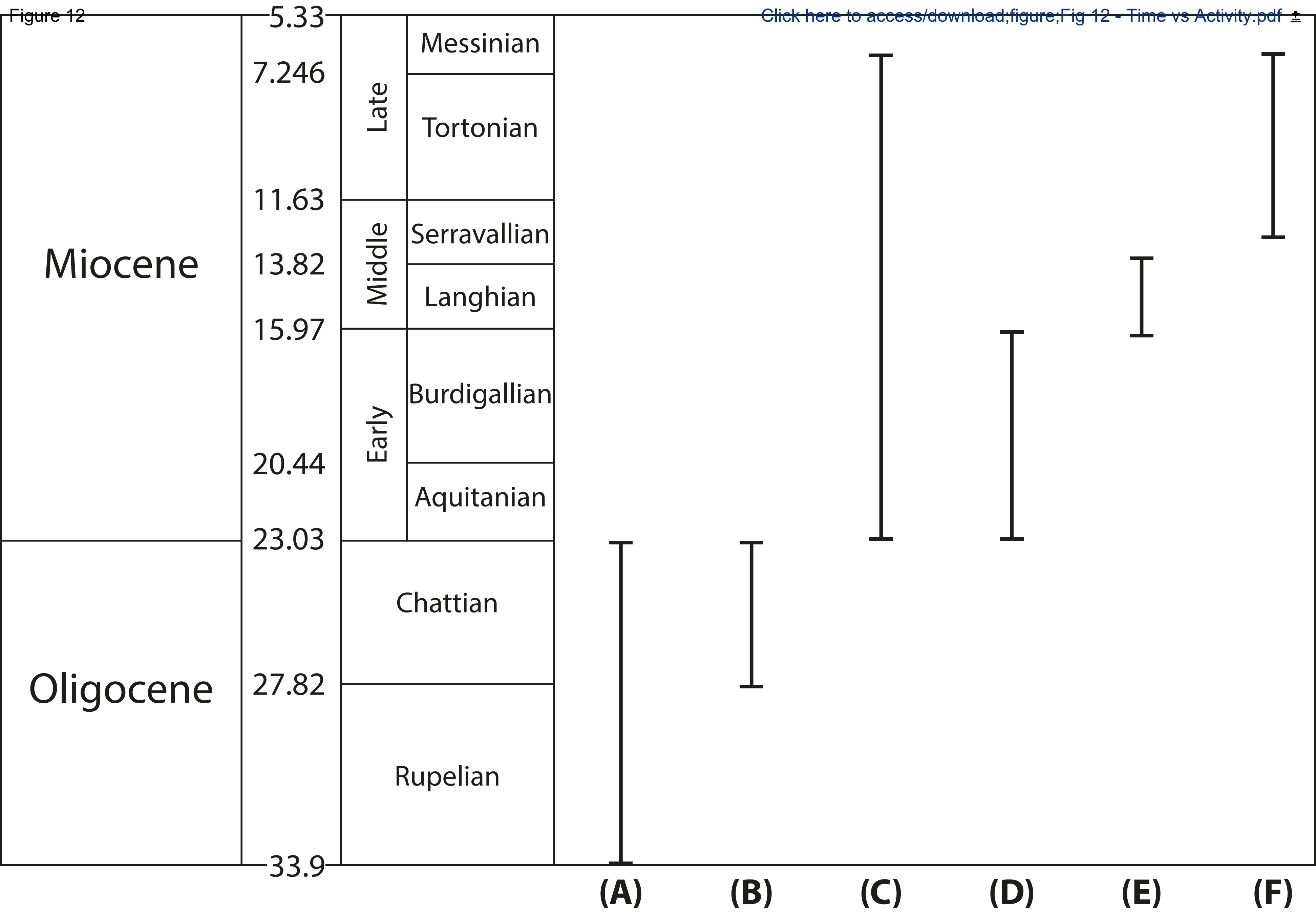
5.33
7.246
11.63
13.82
15.97
20.44
23.03
27.82
33.9
Miocene
Oligocene
Late
Middle
Early
Messinian
Tortonian
Serravallian
Langhian
Burdigallian
Aquitanian
Chattian
Rupelian
(A)
(B)
(C)
(D)
(E)
(F)

Figure 13

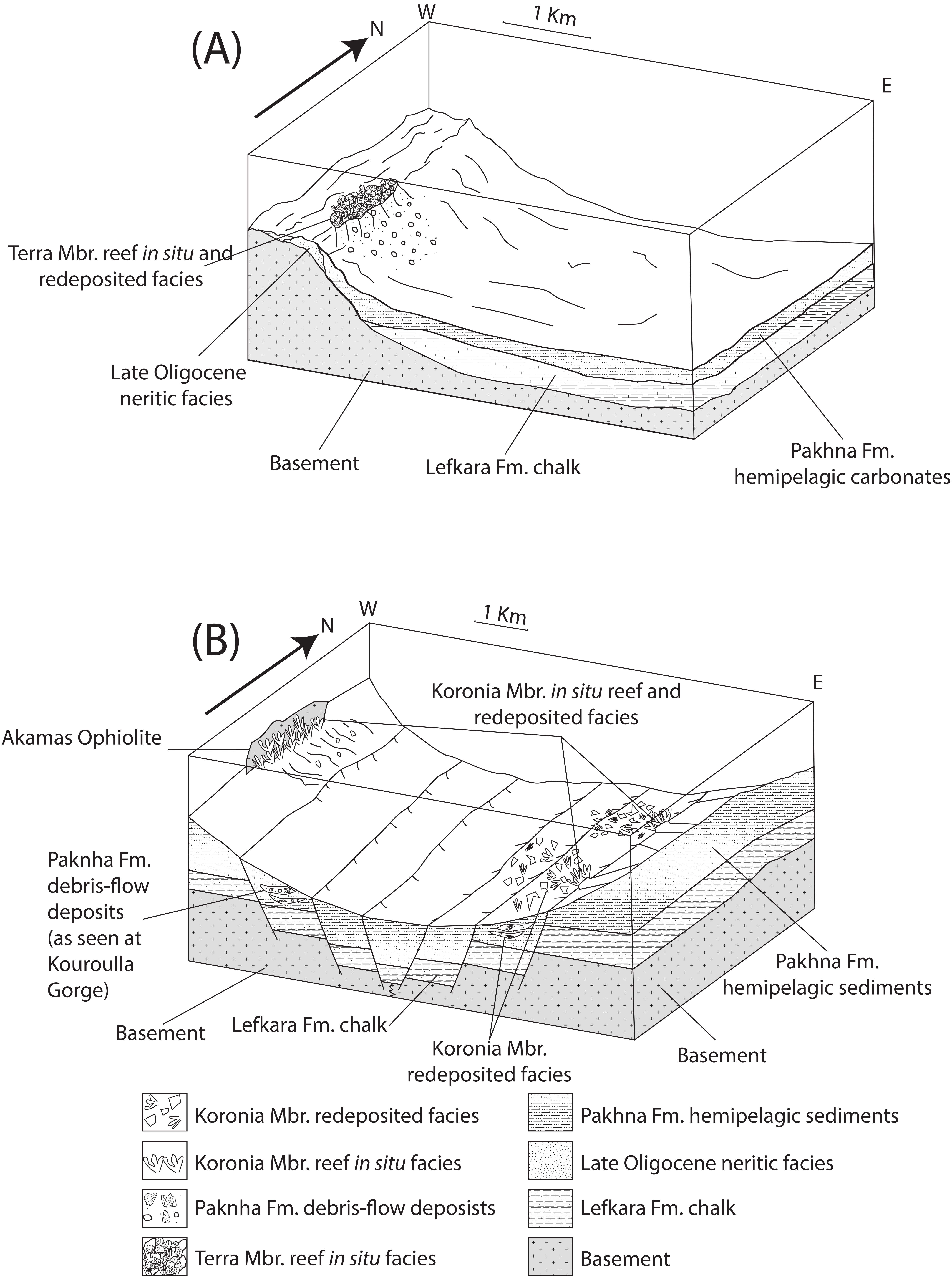
(A)
N
W
1 Km
E
Terra Mbr. reef *in situ* and redeposited facies
Late Oligocene neritic facies
Basement
Lefkara Fm. chalk
Pakhna Fm. hemipelagic carbonates
(B)
N
W
1 Km
E
Koronia Mbr. *in situ* reef and redeposited facies
Akamas Ophiolite
Paknha Fm. debris-flow deposits (as seen at Kouroulla Gorge)
Basement
Lefkara Fm. chalk
Koronia Mbr. redeposited facies
Pakhna Fm. hemipelagic sediments
Basement
Koronia Mbr. redeposited facies
Koronia Mbr. reef *in situ* facies
Paknha Fm. debris-flow deposists
Terra Mbr. reef *in situ* facies
Pakhna Fm. hemipelagic sediments
Late Oligocene neritic facies
Lefkara Fm. chalk
Basement

Figure 14

Click here to access/download

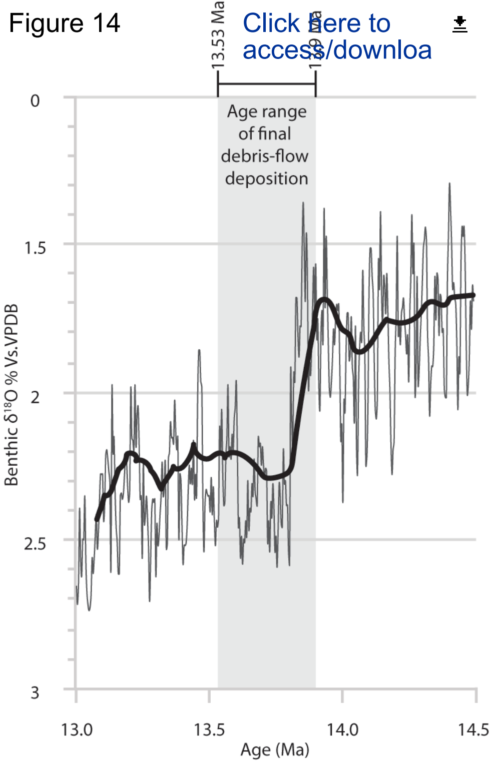

Click here to access/download
supplementary material
TC NW Cyprus MS Supplementary Material.docx